

AD-A187 679

ATMOSPHERIC BACKSCATTER AT 106 MICROMETERS A COMPENDIUM 1/1

OF MEASUREMENTS M. (U) ROYAL SIGNALS AND RADAR

ESTABLISHMENT MALVERN (ENGLAND) J H VAUGHAN ET AL

UNCLASSIFIED

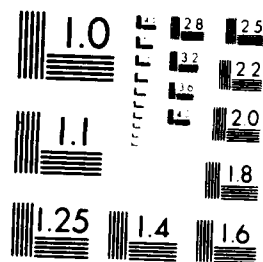
MAY 87 ASKE-87002 DNIC-BN-103339

F/G 1779

NL



END
DATE
288
1779



MAKING COPY RESOLUTION TEST CHART
1963-A

THE FILE COPY

UNLIMITED

DR103339

②

AD-A187 679

Report No. 87002



Report No. 87002

ROYAL SIGNALS AND RADAR ESTABLISHMENT,
MALVERN

ATMOSPHERIC BACKSCATTER AT 10.6 μ m;
A COMPENDIUM OF MEASUREMENTS MADE OUTSIDE THE UNITED KINGDOM
BY THE AIRBORNE LATAS COHERENT LASER RADAR VELOCIMETER

J M Vaughan, D W Brown, P H Davies and R Foord
Royal Signals and Radar Establishment
Great Malvern, Worcs. WR14 3PS, UK

J Cannell, C Nash and A A Woodfield
Royal Aircraft Establishment
Cobham, Bedford. MK41 6AE, UK

D A Bowdle
Johnson Research Center
University of Alabama - Huntsville, AL 35898, USA

J Rothman
Universities Space Research Association
NASA Marshall Space Flight Center
Huntsville, AL 35812, USA

*Original contains color
plates: All DTIC reproductions
will be in black and
white*

DTIC
ELECTE
NOV 04 1987
S E D

PROCUREMENT EXECUTIVE, MINISTRY OF DEFENCE
RSRE
Malvern, Worcestershire.

87 11 3 455 May 1987

UNLIMITED

ROYAL SIGNALS AND RADAR ESTABLISHMENT

Report No 87002

Title: ATMOSPHERIC BACKSCATTER AT 10.6 μm . A COMPENDIUM OF MEASUREMENTS MADE OUTSIDE THE UNITED KINGDOM BY THE AIRBORNE LATAS COHERENT LASER RADAR

Authors: J M Vaughan, D W Brown, P H Davies & R Foord (RSRE UK)
J Cannel, C Nash & A A Woodfield (RAE Bedford, UK)
D Bowdle (University of Alabama, USA)
J Rothermel (NASA, USA)

Date: May 1987

ABSTRACT

Over 30 hours of airborne measurement of the atmospheric backscatter coefficient $\beta(\pi)$ at 10.6 μm are reported, for four different regions of the Northern Hemisphere outside the UK, at altitudes up to 13 km. The results exhibit great diversity. In several recordings $\beta(\pi)$ remains constant within a factor of three over large distances and height intervals; in others over four orders of magnitude change is observed. The value of $\beta(\pi)$ rarely falls below the sensitivity limit of the equipment of $\sim 2.2 \times 10^{-11} \text{ m}^{-1} \text{ sr}^{-1}$. If such findings are typical of the atmosphere as a whole they strongly support the conclusion that 1) airborne laser radars for the measurement of true airspeed, and wind shear detection and warning at low levels, would have good reliability and 2) a Laser Atmospheric Wind Sounder (LAWS) for global wind field measurement would provide reliable information for a very large fraction of the time.

Original sent to color
photo by APTD repro-
duced in black and
white

Copyright
C
Controller HMSO London
1987

Accession For	
NTIS SP&I	<input checked="" type="checkbox"/>
DTIC TAB	<input checked="" type="checkbox"/>
Unannounced	<input type="checkbox"/>
Justification	
By	
Distribution/	
Availability Codes	
Dist	Avail and/or Special
A-1	

1. INTRODUCTION

The airborne **LA**ser **T**ru \mathbf{e} **A**ir **S**peed (LATAS) system designed and built at RSRE has been operated in a flying programme in the HS125 aircraft at RAE Bedford for the five years 1981-6. The equipment operates by heterodyne measurement of the relative Doppler shift between the transmitted laser frequency and return radiation scattered by atmospheric aerosols. The LATAS system has been described in several articles, and studied in various flight trials including measurement of true airspeed, advance detection and warning of wind shear and microbursts, and pressure error calibration [1,2]. An additional and important part of the flight programme has been measurement of the atmospheric backscatter coefficient $\beta(\pi)$ which is defined as the fraction of the incident laser energy scattered from a 1 m path along the beam into unit solid angle in the backward direction (and thus has the units $\text{m}^{-1} \text{sr}^{-1}$). Values of $\beta(\pi)$ may be derived from the magnitude of the Doppler signal and the calibration factor of the equipment.

This report summarizes measurements made during flights outside the United Kingdom; corresponding measurements within the UK will be presented in a later publication. The present compendium thus includes a sequence of flights across the Arctic to North America and return in June/July 1982, ten flights in Colorado in June/July 1982 during the JAWS (Joint Airport Weather Studies) programme, three tours to Gibraltar in December 1981, June 1982 and February 1983 and a brief visit to Norway and into the Arctic Circle in March 1986. Measurements were made during climbs to the maximum altitude of the aircraft (~ 13 km), in transit flights at constant altitude over several hundred kilometres, and on most descents. The results are shown as a sequence of diagrams with $\beta(\pi)$, static air temperature, altitude and time variously plotted.

The purpose of compiling these backscatter measurements has been two fold: firstly to establish an envelope of reliable performance for aircraft operation with measurement of true airspeed by laser Doppler scattering from aerosols. The second aim has been to investigate atmospheric back-scattering as widely as possible in order to provide a data base for evaluation of a satellite born Laser Atmospheric Wind Sounder (LAWS) - which has also been called the Wind Profiling Lidar (WPLID). Such laser based equipments to provide measurements of the Global Wind Field are presently being considered for purposes of meteorology, atmospheric dynamics and improved weather forecasting.

2. THE EQUIPMENT AND SIGNAL RECORDING

A complete block diagram of the LATAS airborne laser radar is shown in Figure 1. The HS125 aircraft and the optics head in its nose are shown in Figure 2. The radiation source is a 3 watt continuous wave CO_2 laser controlled to operate on the P20 transition at $10.6 \mu\text{m}$. The laser beam is transmitted from a 150 mm diameter telescope lens and for backscatter measurements is usually set to focus at 100 m range to give a depth of focus of about ± 15 m (ie this, together with the

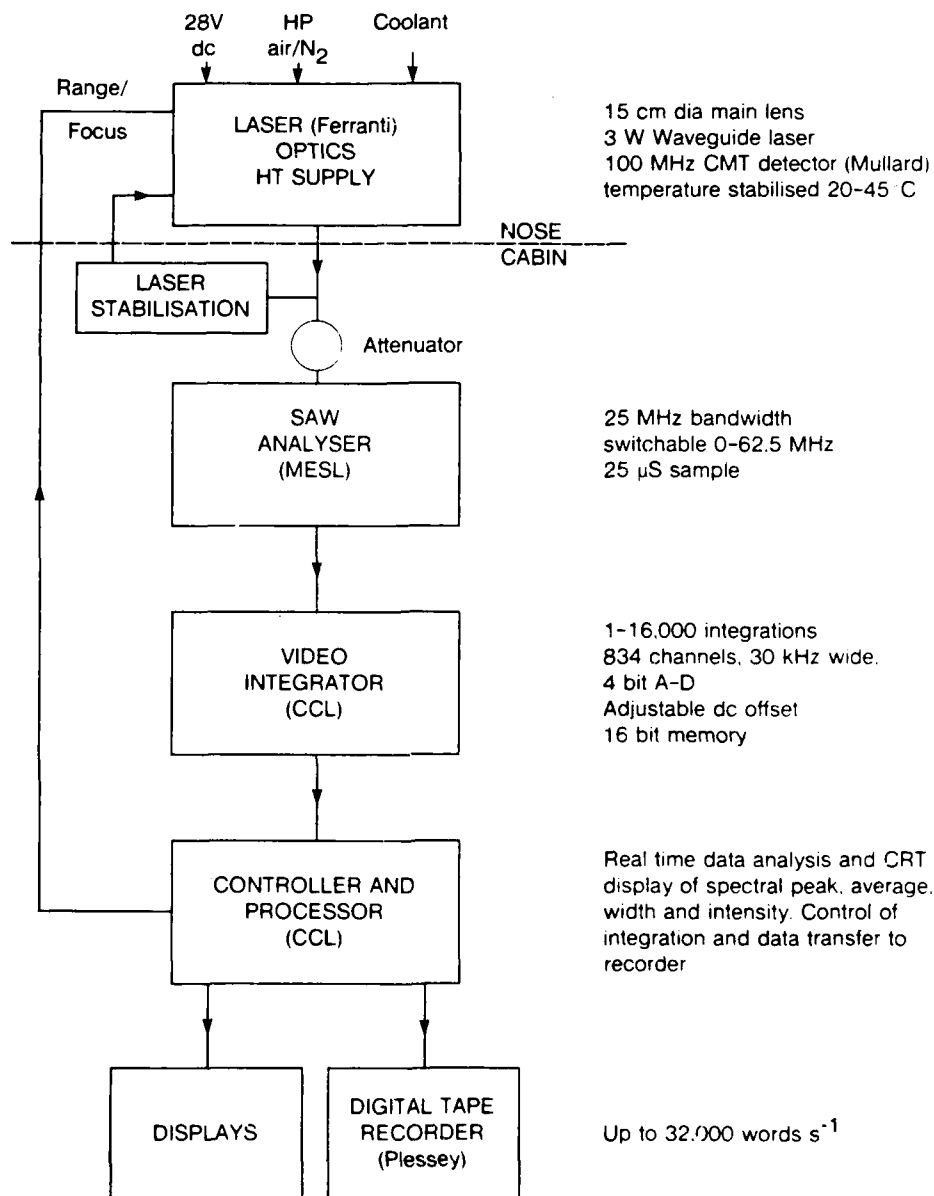
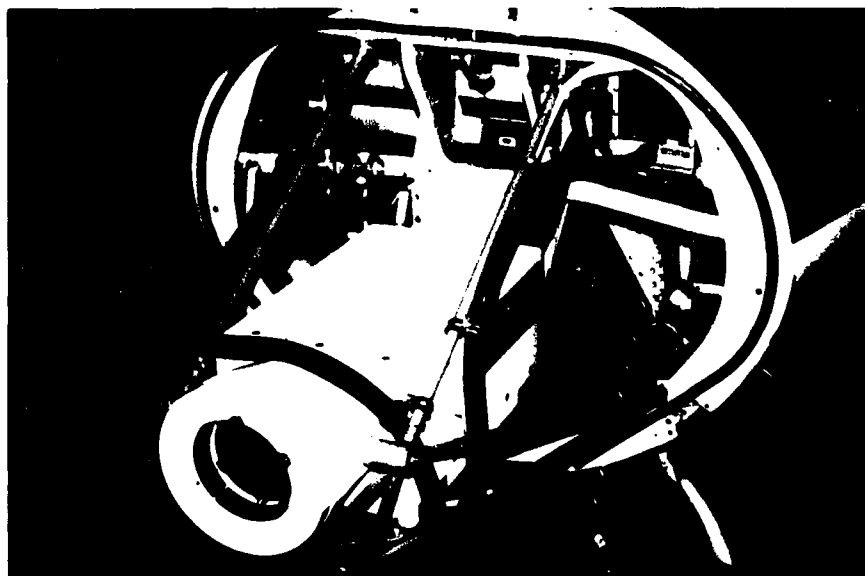


Figure 1. Block Diagram of the Airborne CO₂ Laser Velocimeter Equipment (LATAS).



2a. HS125 Aircraft



2b. Optics Head

Figure 2. The RSRE/RAE Airborne CO₂ Laser Velocimeter (LATAS)

beam diameter of ~ 10 mm at focus, defines the pencil-like probe volume from which the bulk of the aerosol scattering emerges). Scattered radiation re-enters the system and is mixed with an optical local oscillator derived from the original laser beam. Heterodyne detection takes place at a CMT photodiode. Signal processing equipment is installed in the cabin of the aircraft and of the resultant electrical signal, samples $25 \mu\text{s}$ long are frequency analysed by a surface acoustic wave spectrum analyser which outputs the spectra of successive samples to an A/D converter and integrator. These individual Doppler spectra are then built up in the integrator and are recorded with instrument and flight data on a tape recording system. Complete spectra can be recorded at rates up to 15 Hz but the backscatter measurements were usually recorded every few seconds over an experimental period in the range 0.2 to 0.8 s with up to 12×10^3 samples accumulated in the integrator to improve the observed signal to noise ratio.

3. DERIVATION OF BACKSCATTER VALUES $\beta(\pi)$

The calibration of the coherent laser radar, and the derivation of an expression for the backscatter coefficient $\beta(\pi)$ in the system is discussed at length in references [3] and [4].

In summary $\beta(\pi)$ is given by

$$\beta(\pi) = [3.32 \times 10^{-10}/P_0] [(SNR_V) [k(m_1 - m_0)]^{1/2}/(K) + 1^2 - 1] \quad \dots\dots 3.1$$

where the likely limit of error on the numerical term is $\sim 1\frac{1}{2}$ dB (a factor ~ 1.4) and P_0 is the actual transmitted power of the laser beam. The mean observed SNR_V due to a single sample is given by

$$SNR_V = \sum_{m=m_0}^{m_1-1} \sigma_s(m) / (m_1 - m_0)^{1/2} \sigma_n \quad \dots\dots 3.2$$

and $k = 0.273$ and $K \approx 1$. The summation is over the number of channels $(m_1 - m_0)$ containing detectable signals $\sigma_s(m)$, and σ_n is the root variance of the noise background.

In practice the computational algorithm that takes tape recorded data and calculates values of $\beta(\pi)$ is quite complex; it is described in detail in reference [5]. It incorporates many factors that include synchronous noise, sloping noise background etc. In the presence of strong backscatter the Doppler peak is obvious and may be determined without ambiguity. For small signals however, typically $< 5 \times$ root variance of the noise, a random wide-ranging search across the spectrum could produce spurious peaks. Use of a narrow search window is a valuable safeguard against this problem; such a search window is provided by the calculated airspeed V_t derived from the on-board

pitot-static head and the air data computer. The search window is usually defined as $V_t \pm 3$ knots; in fact the difference between the laser airspeed S_p (after correction for aircraft angle of attack, laser rigging angle etc) and V_t provides a valuable diagnostic as illustrated for Flt No 761 in Section 5. With these procedures signal peaks down to $\sim 2.5 \times$ root variance of the noise can be extracted in practice with an acceptably small chance of recording a false signal.

With reference to equation 3.1 the minimum value of $\beta(\pi)$ that can be obtained is $\approx 2.2 \times 10^{-11} \text{ m}^{-1} \text{ sr}^{-1}$ for a full 12×10^3 integrations. Equation 3.1 with $K = 1$ provides a good approximation for small signals and $\beta(\pi) < 10^{-9} \text{ m}^{-1} \text{ sr}^{-1}$. At higher values there is some tendency to overestimate $\beta(\pi)$ but this is counteracted in practice by the limited dynamic range of the signal processing equipment (see reference [4]).

4. THE AIRBORNE MEASUREMENTS

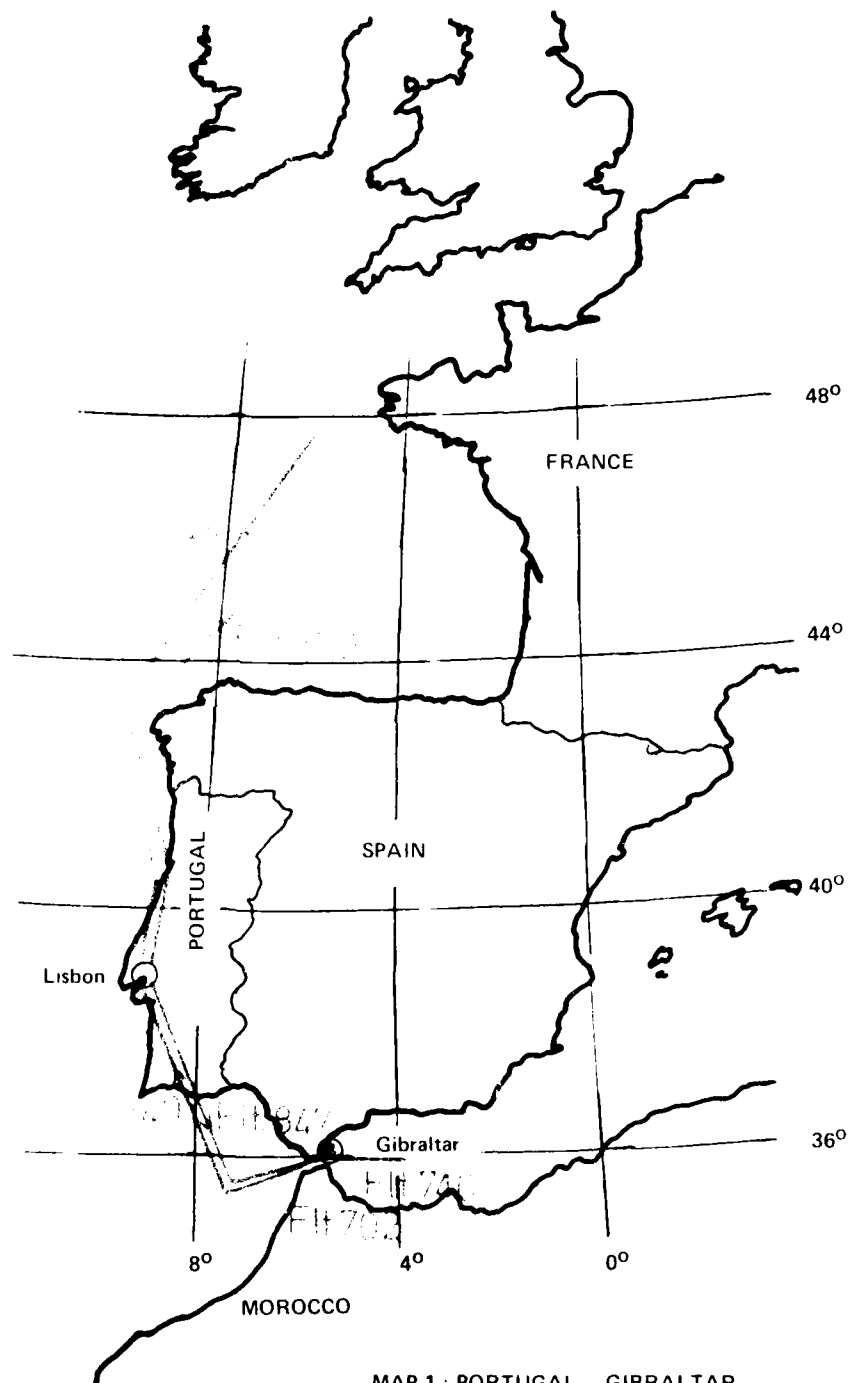
The approximate location of each of the flights is shown on Maps 1-4. For convenience the measurements are presented in four groups as follows:

a) FLIGHTS OFF GIBRALTAR (MAP 1)

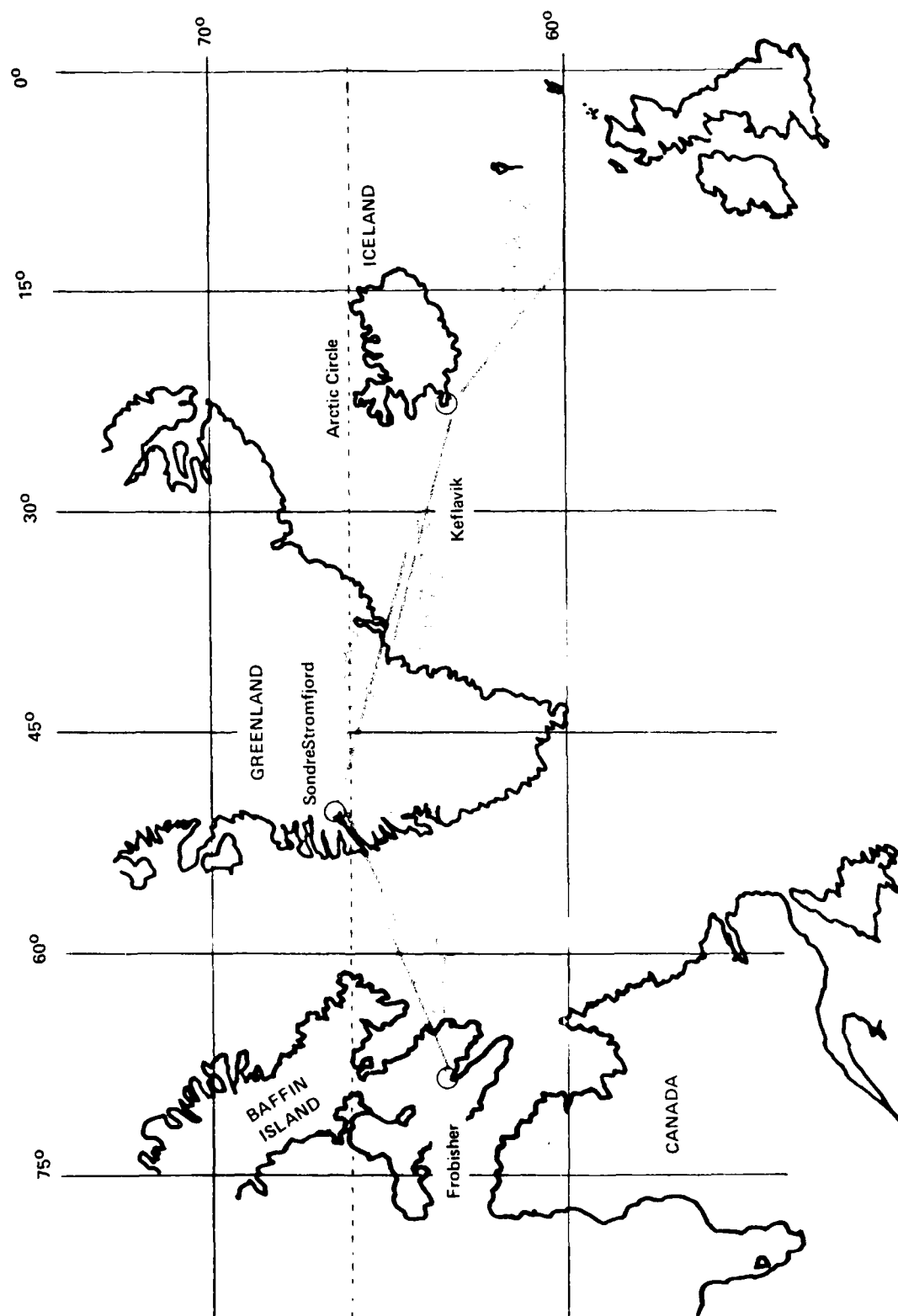
- 1 Flight 702: 4 Dec 1981; climb out of Gibraltar (figure 3 A, B)
- 2 Flight 740: 4 Jun 1982; climb out of Gibraltar (figure 4 A, B)
- 3 Flight 744: 7 Jun 1982; climb and transit Lisbon-north (figure 5 A, B)
- 4 Flight 847: 9 Feb 1983; climb and transit Lisbon-Gibraltar (figure 6 A, B)
- 5 Flight 849: 12 Feb 1983; climb and transit Gibraltar-Lisbon (figure 7 A, B)
- 6 Flight 850: 12 Feb 1983; climb and transit Lisbon-north (figure 8 A, B)

b) FERRY FLIGHTS: ICELAND-GREENLAND-NORTH AMERICA (MAPS 2, 3)

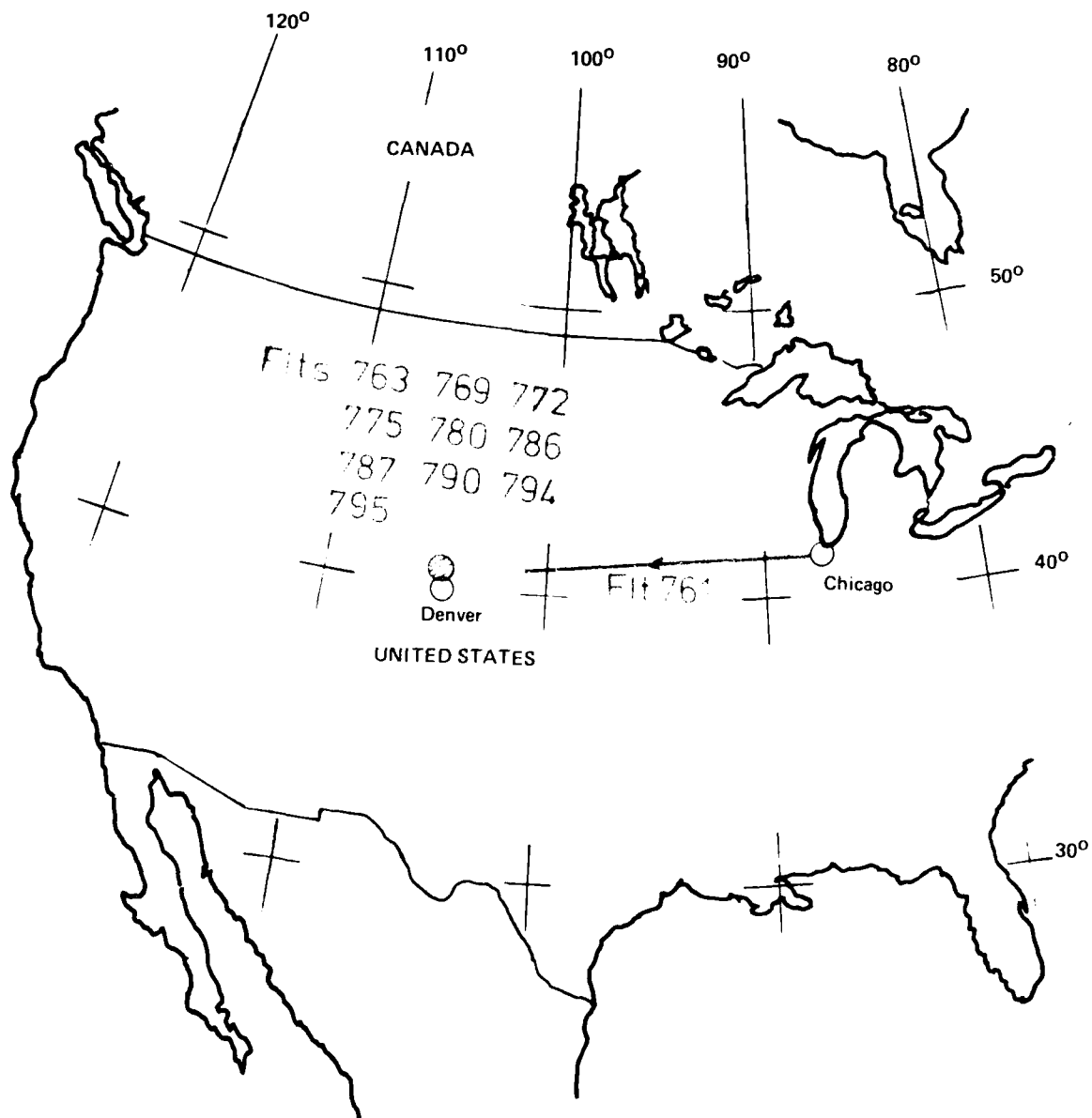
- 1 Flight 757: 22 Jun 1982; climb and transit Keflavik-SondreStromfjord (figure 9 A, B)
- 2 Flight 758: 22 Jun 1982; climb and transit SondreStromfjord-Frobisher (figure 10 A, B)
- 3 Flight 761: 24 Jun 1982; climb and transit Chicago-Denver (figure 11 A, B)
- 4 Flight 800: 19 Jul 1982; climb and transit Frobisher-SondreStromfjord (figure 12 A, B)
- 5 Flight 801: 19 Jul 1982; climb and transit SondreStromfjord-Keflavik (figure 13 A, B)
- 6 Flight 802: 20 Jul 1982; climb and transit Keflavik-Lossiemouth (figure 14 A, B)



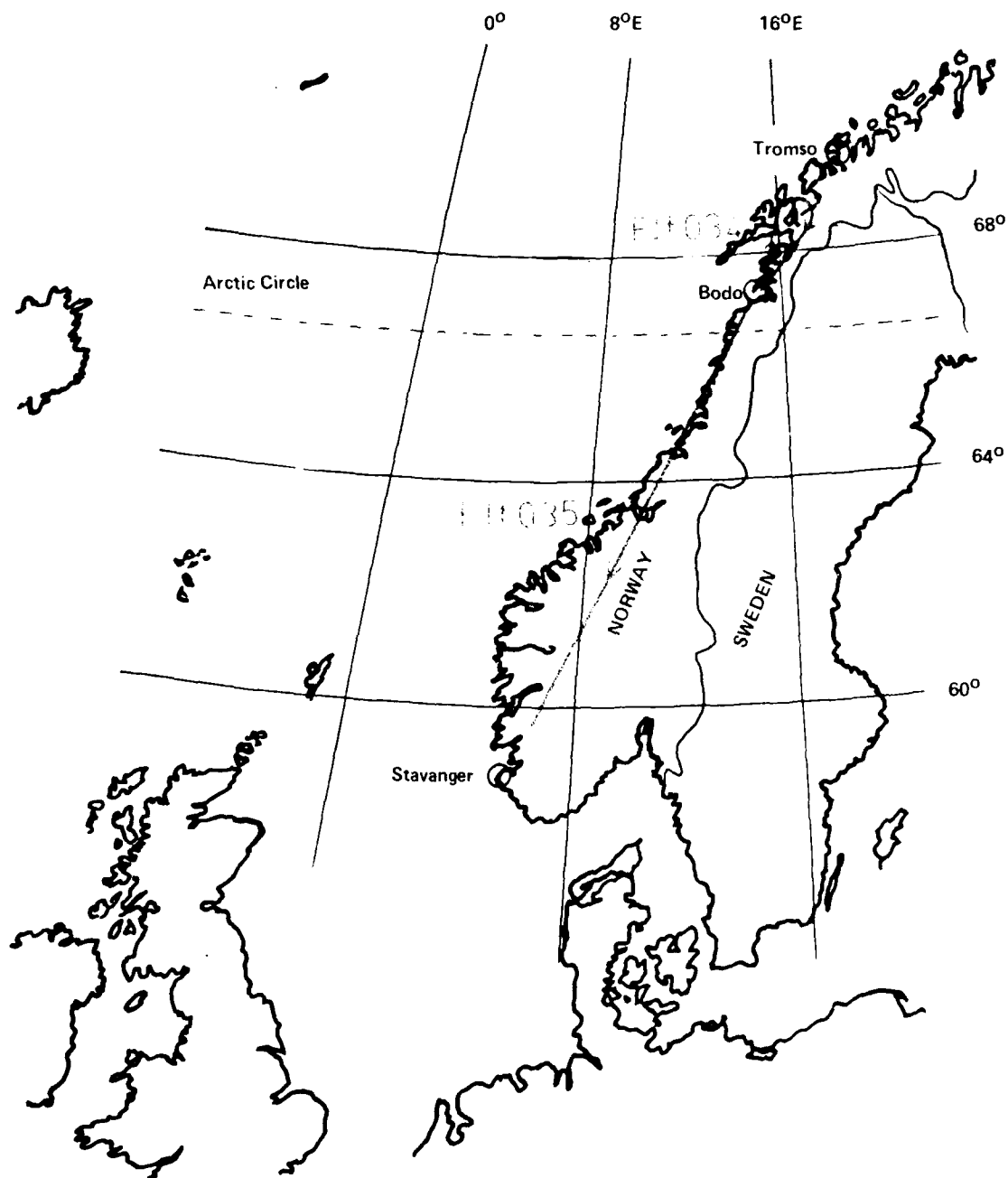
MAP 1 : PORTUGAL - GIBRALTAR



MAP 2 : ICELAND - GREENLAND



MAP 3 : NORTH AMERICA



MAP 4 : NORWAY - ARCTIC CIRCLE

c) MEASUREMENTS DURING JAWS, COLORADO JUNE-JULY 1982 (MAP 3)

(all climbs out of Jefferson County Airport, Colorado, height 1.7 km ASL, usually followed by rapid descent.)

- 1 Flight 763 28 Jun 1982 (figure 15 A, B)
- 2 Flight 769 1 Jul 1982 (figure 16 A, B)
- 3 Flight 772 2 Jul 1982 (figure 17 A, B)
- 4 Flight 775 7 Jul 1982 (figure 18 A, B)
- 5 Flight 780 9 Jul 1982 (figure 19 A, B)
- 6 Flight 786 12 Jul 1982 (figure 20 A, B)
- 7 Flight 787 13 Jul 1982 (figure 21 A, B)
- 8 Flight 790 14 Jul 1982 (figure 22 A, B)
- 9 Flight 794 15 Jul 1982 (figure 23 A, B)
- 10 Flight 795 16 Jul 1982 (figure 24 A, B)

d) FLIGHTS OFF NORWAY MARCH 1986 (MAP 4)

- 1 Flight 034 19 March 1986 (cont. and trans B) (cont. and trans B) (cont. and trans B)
- 2 Flight 035 19 March 1986 (cont. and trans B) (cont. and trans B) (cont. and trans B)

Values of ρ_{m} and Static Air Temperature are plotted against aircraft altitude for the first part of each flight (figures A); the facing pages (figures B) show the available records of transmittance plotted for the same flights with ρ_{m} and altitude plotted against time. Notes from the flight observer, together with comments on various features of the measurements are given below each figure.

In consideration of these records several points arise from their preparation and the experimental operation. In practice the flight observer has a heavy work load starting with the switch on, the monitoring of many diagnostic readouts and matching of various experimental parameters to the atmospheric conditions and aircraft speed. This latter point can present particular difficulties. In general it was found that most reliable operation could be obtained by presetting the receiver (attenuation, offsets, number of integrations, focus) for the particular conditions of interest. This of course would not necessarily be ideal for other unexpected conditions and occasional minor changes, usually of gain or number of integrations, would have to be made. Small gaps in the data arise from many possible causes and include

- a) Genuine loss of signal due to low backscatter strength, with no signal peak found at the end of the analysis criteria (see also the discussion in following section)

- b) Lost-lock on the laser and reduced sensitivity.
- c) Occasional short-lived icing up of the transmitting window - a rare occurrence usually on sharp descent from high altitude into cloud.
- d) An excessively strong signal which has saturated and overloaded the detector and/or recording system.
- e) The spectral peak appearing too close to the end of the spectrum so that background noise cannot be evaluated.
- f) Corrupted data due to a transcription error in the tape recorder and reader.
- g) Change of experimental parameter during the measurement.

Wherever possible such causes have been identified and noted on the figures. In particular the letters 'm' and 's' have usually been assigned to regions where the signals fell close to or below the minimum detectable (m) and where saturation occurred (usually, but not always, in cloud) (s).

5. DISCUSSION

Consideration of the whole body of data shows that only Flt 702 and Flt 740 near Gibraltar present major problems. These were the two earliest flights carried out before the best procedures had been established and the equipment was not operated at optimum sensitivity (with the largest possible number of integrations). For Flt 702 there is also indication of a malfunction that may have further reduced system sensitivity. In view of these considerations these two flights have been excluded from the following analysis.

Inspection of the remaining 22 flights shows the following broad features:-

- 1 'Strong' backscattering with $\beta(\pi) > 5 \times 10^{-10} \text{ m}^{-1} \text{ sr}^{-1}$ is invariably found at low altitudes less than 2 km AGL.
- 2 Such 'strong' backscattering [$\beta(\pi) > 5 \times 10^{-10} \text{ m}^{-1} \text{ sr}^{-1}$] occurs for at least 60% of the record throughout the troposphere.
- 3 Sharp reductions of backscatter (up to two orders of magnitude) are often associated with even minor temperature inversions and may occur over very narrow height intervals. Similarly very large increases in backscattering can occur over very narrow height intervals and are usually associated with sub-visible cirrus.

- 4 Backscatter levels usually fall to a minimum at 8 to 10 km with typical values of $\beta(\pi) < 10^{-10} \text{ m}^{-1} \text{ sr}^{-1}$.
- 5 Above 10 km the backscattering usually increases with altitude particularly for penetration into the stratosphere. Usually there are no very obvious changes of backscatter level at the tropopause.
- 6 Backscatter levels falling below the minimum detectable value of $\beta(\pi) \approx 2.2 \times 10^{-11} \text{ m}^{-1} \text{ sr}^{-1}$ are comparatively rare and occupy less than $\sim 1\%$ of the record. During climbs they rarely persist over height intervals greater than a few tenths of a kilometre. In level flight they rarely persist more than a few tens of kilometres.

In relation to this final point, and the general problems of low signal, inspection of the flight records show that the only extended period (~ 12 minutes corresponding to ~ 100 km path) for which the backscatter was at a consistently low level occurs in Flight 761 (figure 11 B) for the time 47-59 minutes. In fact for this flight (and a number of other lengthy transits, eg Flts 801 and 802) the equipment was set up with 4×10^3 integrations per measurement to give a minimum detectable backscatter level of $\sim 3.8 \times 10^{-11} \text{ m}^{-1} \text{ sr}^{-1}$. Thus the system was not operating at maximum sensitivity. Nevertheless a number of diagnostic tests (figures 27-29) were carried out on this piece of data to investigate whether an equipment malfunction could be responsible for the low signal observed in the 12 minute period. The background noise level is plotted in figure 27 and shows no anomalies; this establishes that the optical local oscillator and laser power were at the correct level and the equipment should have been fully sensitive throughout the recording. However, the bimodal distribution of the $\beta(\pi)$ points evident for this 12 minute time interval in figure 11 B (with separation at $\sim 2 \times 10^{-11} \text{ m}^{-1} \text{ sr}^{-1}$), which also appears on a number of other records, is somewhat puzzling. In an effort to identify the source of this anomaly, the allowed search window was narrowed to ± 1.5 knots from the standard ± 3 knots, with the result shown in figure 28. However, the result was very little changed and the bimodal distribution remained (compare figures 28 and 11 B).

The interpretation of this bimodal structure lies in equations 3.1 and 3.2, the discrete sampling over 30 kHz channels in frequency space, and the criteria for accepting a signal peak. Consider the threshold to be set at a low value (eg 'signal' peak only $> 2.5 \times \text{rms noise}$); one or more adjacent channels may register as 'signal'. If only one channel registers just above threshold it will appear to give a very low backscatter level but in fact has a very low probability of being genuine. If two adjacent channels register just above threshold the apparent backscatter level is approximately doubled (hence the bimodal character), and the probability of being a genuine measurement is somewhat improved, at least for measurements with many integrations. Setting a much higher threshold (eg $> 5 \times \text{rms noise}$) would of course almost totally eliminate the chance of recording spurious data points but would also lose many genuine measurements. These questions will be discussed at greater length in a later paper. For present purposes a very low threshold ('signal' $> 2 \times \text{rms noise}$) has been adopted in order to explore the lowest possible backscatter signal levels. Correspondingly the data must be interpreted with caution — any data point below $\sim 10^{-11} \text{ m}^{-1} \text{ sr}^{-1}$

is very unlikely to be genuine; above $2 \times 10^{-11} \text{ m}^{-1} \text{ sr}^{-1}$ the probability of finding spurious data rapidly decreases for measurements based on a full 12×10^3 integrations.

This point is further illustrated by the corresponding plots of $S_p - V_t$ given in figure 29. The small values of $S_p - V_t$ show that for level flight with $\beta(\pi) > 5 \times 10^{-11} \text{ m}^{-1} \text{ sr}^{-1}$ the Doppler peak has been determined with absolute confidence (note the $S_p - V_t$ plots for Elapsed Time > 60 min, and refer to figures 28 and 11 B). However for the interval 47-59 minutes the $S_p - V_t$ points are distributed almost randomly across the search window with only slightly increased density close to the $S_p - V_t = 0$ regression line. We may conclude that in the absence of any extraneous effects (eg icing up of a transmitting window — of which there is no suggestion in the observer's log) the backscatter throughout this 12 min interval was most of the time at or below the appropriate maximum sensitivity level of $\sim 3.8 \times 10^{-11} \text{ m}^{-1} \text{ sr}^{-1}$.

As a final point it is worth noting that the only contemporary particle counting measurement was made during Flt 790 and showed a very low count rate for backscatter levels around $10^{-10} \text{ m}^{-1} \text{ sr}^{-1}$. This single comparison hardly merits much interpretation but might suggest that backscattering at $10.6 \mu\text{m}$ at such levels is dominated by the integration of scatter from numbers of small particles of size considerably less than $1 \mu\text{m}$.

6. CONCLUSION

At this stage no attempt has been made to relate all the measurements to the local meteorology and general climatology. For the full body of data this would present a massive task and is currently only being carried out for the JAWS flights and comparable and contemporary data from the ground-based pulsed laser radar of the NOAA Wave Propagation Laboratory [6].

The results given in the foregoing figures are for measurements widely separated in space and time. The most important findings would seem to be that:

- 1) 'strong' backscattering with $\beta(\pi) > 5 \times 10^{-10} \text{ m}^{-1} \text{ sr}^{-1}$ is invariably found at low altitudes less than 2 km AGL and occurs for about 60% of the time through the troposphere.
- 2) Backscatter values falling below $\beta(\pi) \sim 2 \times 10^{-11} \text{ m}^{-1} \text{ sr}^{-1}$ are comparatively rare, occupying less than $\sim 1\%$ of the total observation time.

If these findings are reasonably typical of atmospheric backscattering for the regions observed during the period, and if duplicated in other parts of the globe, they would suggest that airborne laser radars, operating at low altitudes for measurement of true airspeed and wind shear detection and warning, would have good reliability. Furthermore a satellite borne Laser Atmospheric Wind

Sounder (LAWS) for global wind measurement and with a maximum sensitivity for backscatter of $\sim 2 \times 10^{-11} \text{ m}^{-1} \text{ sr}^{-1}$ would provide reliable information for a very large fraction of the time.

ACKNOWLEDGEMENTS

We are indebted for the assistance of many colleagues and the enthusiastic cooperation of air and ground crew throughout this extended programme of work. We particularly wish to thank R Callan, G D J Constant, R Jones, C Roberts and D V Willets at RSRE, and also D Bull of RAE Bedford for assistance with the data reduction.

REFERENCES

- [1] A A Woodfield and J M Vaughan.
Airspeed and Wind Shear Measurements with an Airborne CO₂ CW Laser.
Int. J. Av. Safety 1, 207 (1983).
- [2] J M Vaughan and A A Woodfield.
Wind Measurement with Coherent Laser Radar at 10 μm .
Proc. ESA Workshop on Space Laser Applications and Technology, ESA SP-202, 231.
(1984).
- [3] R Foord, R Jones, J M Vaughan and D V Willets.
Precise Comparison of Experimental and Theoretical SNRs in CO₂ Laser Heterodyne Systems.
Appl. Opt. 23, 3787 (1983).
- [4] J M Vaughan, D A Bowdle, R Callan and J Rothermel.
Spectral Analysis, Digital Integration and Measurement of Low Backscatter in Coherent Laser Radar.
(To be published 1987.)
- [5] J Rothermel, D A Bowdle, D W Brown, D Bull, J M Vaughan and A A Woodfield.
Algorithm to Calculate Aerosol Backscatter from Airborne CW Focussed CO Doppler Lidar Measurements.
(To be published 1987.)
- [6] D A Bowdle, D W Brown, M J Post, J Rothermel, J M Vaughan.
Spatial and Temporal Variability of Aerosol Backscatter at 10.6 μm over the Colorado High Plains during JAWS.
(To be published 1987.)

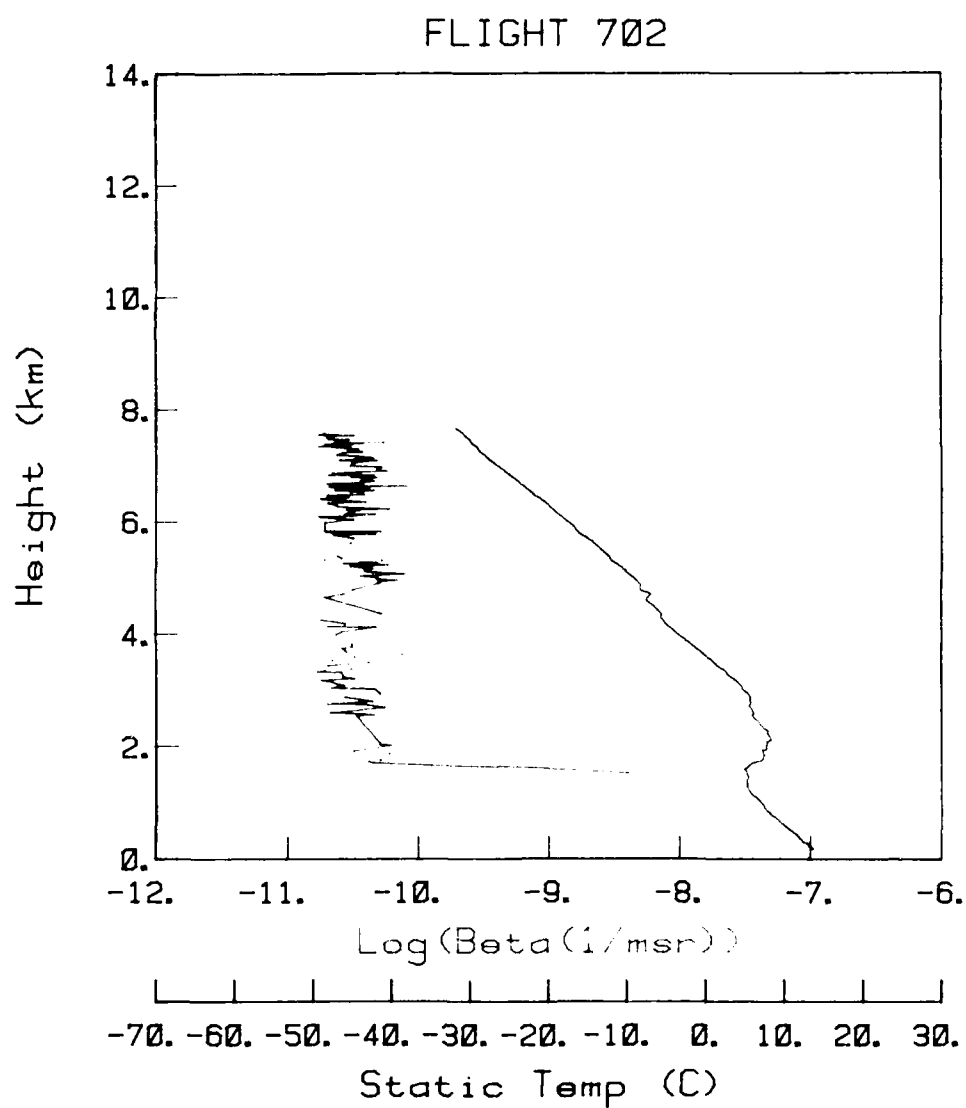


Figure 3A. Climb out of Gibraltar, 4 December 1981. The observer's log records cloud to ~ 1.5 km. In this early flight the number of integrations per measurement was set at only 4×10^3 to give a minimum detectable $\beta(\pi) \approx 4 \times 10^{-11} \text{ m}^{-1} \text{ sr}^{-1}$; above 2 km the backscattering fluctuated around this value

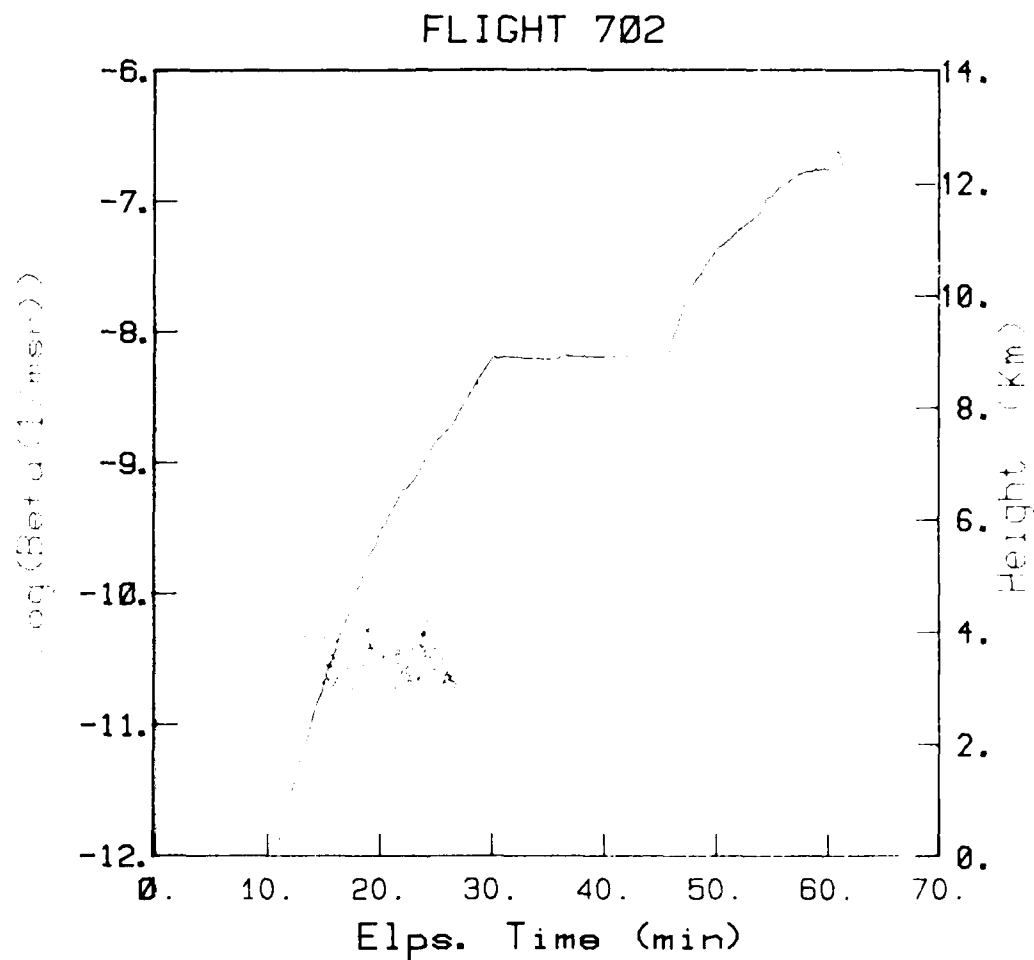


Figure 3B. Climb and transit near Gibraltar, 4 December 1981. The number of integrations per measurement was set at 4×10^3 to give a minimum detectable $\beta(\pi) \approx 4 \times 10^{-11} \text{ m}^{-1} \text{ sr}^{-1}$. Apparently after 27 min the backscatter level fell below this value and is not recorded. However, the observer's log records that "TV (display) threshold fell to half" at about this time. This may indicate a severe equipment malfunction (eg loss of signal amplification, laser power or more likely laser lock) and consequent gross reduction of system sensitivity.

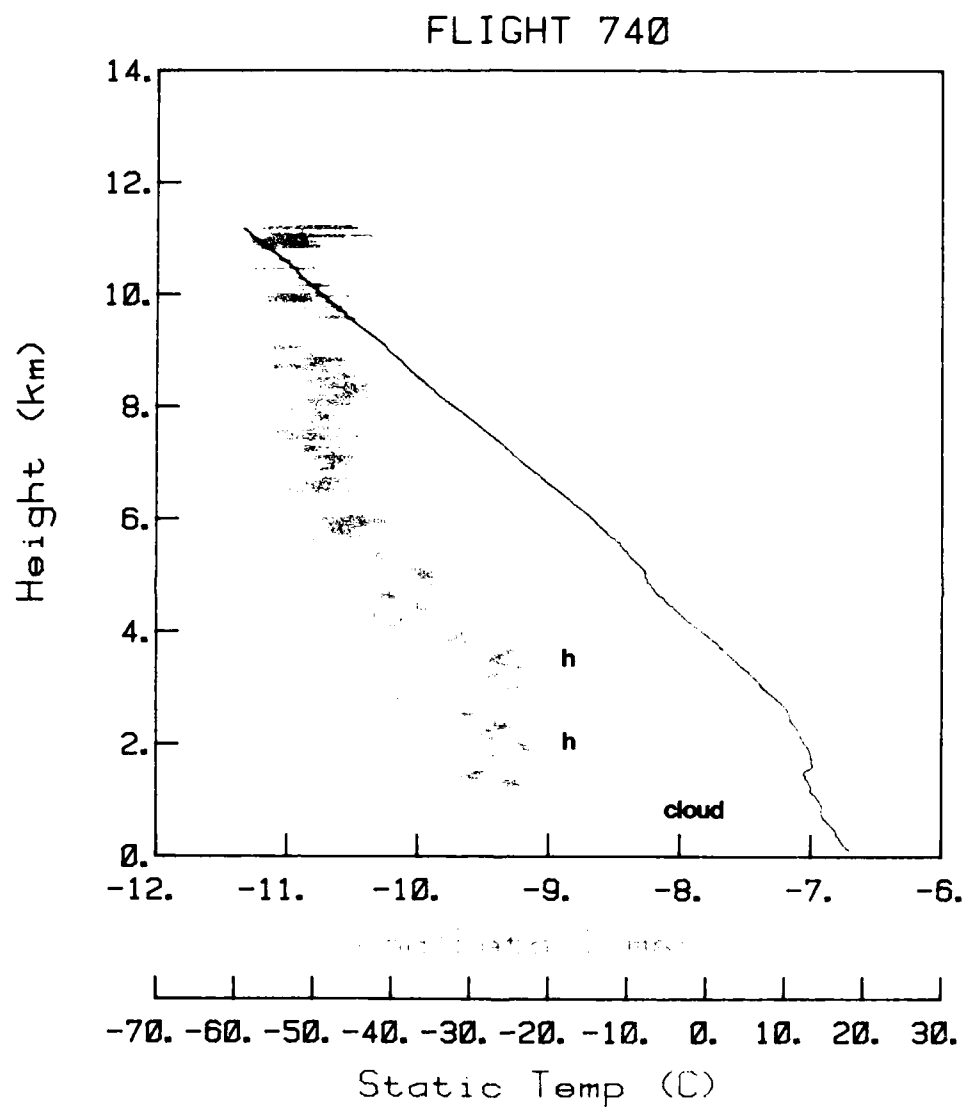


Figure 4A. Climb out of Gibraltar, 4 June 1982. The observer's log records various haze layers (h) to ~ 4 km and low signal above that. During this flight the number of integrations per measurement was 6×10^3 to give a minimum detectable $\beta(\pi) \approx 3 \times 10^{-11} \text{ m}^{-1} \text{ sr}^{-1}$; above 6 km the backscattering fluctuated around this value.

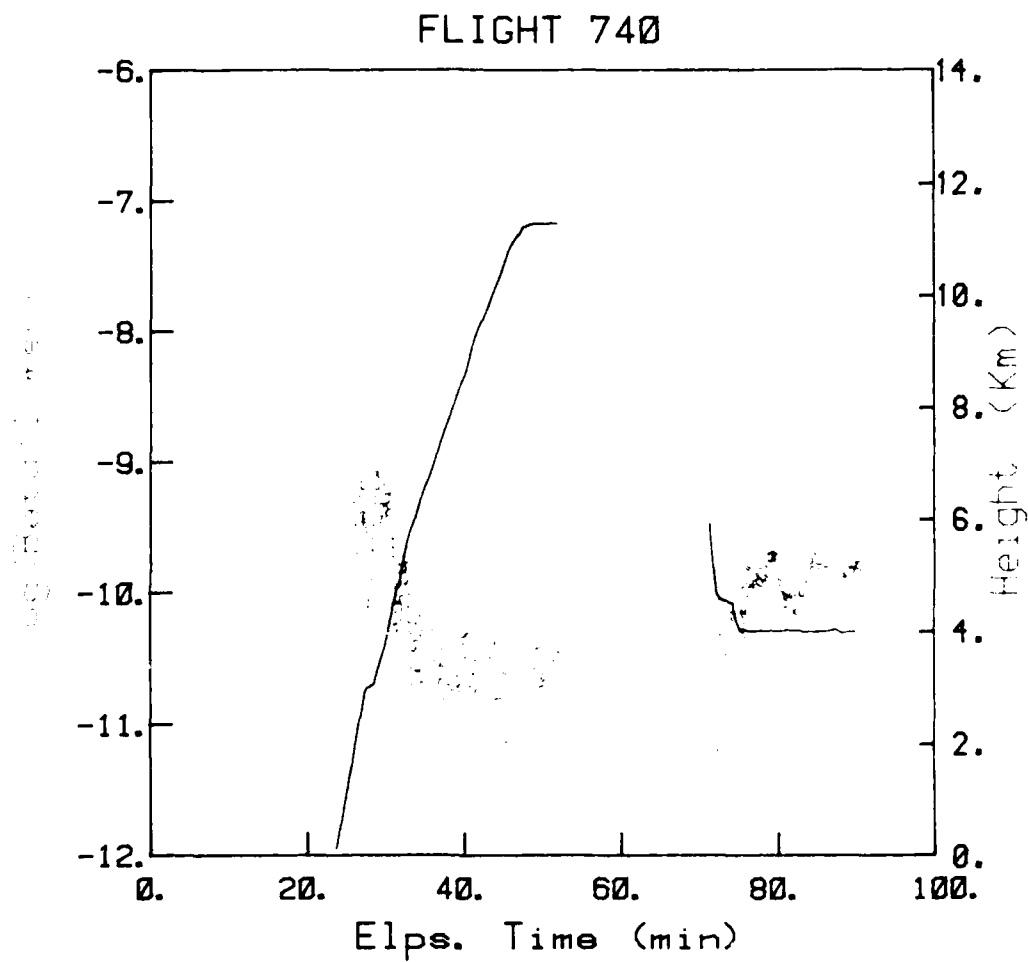


Figure 4B. Climb and transit near Gibraltar, 4 June 1982. Data was not recorded for the period 52-72 min. It is likely that the backscattering above 6 km fluctuated around $3 \times 10^{-11} \text{ m}^{-1} \text{ sr}^{-1}$.

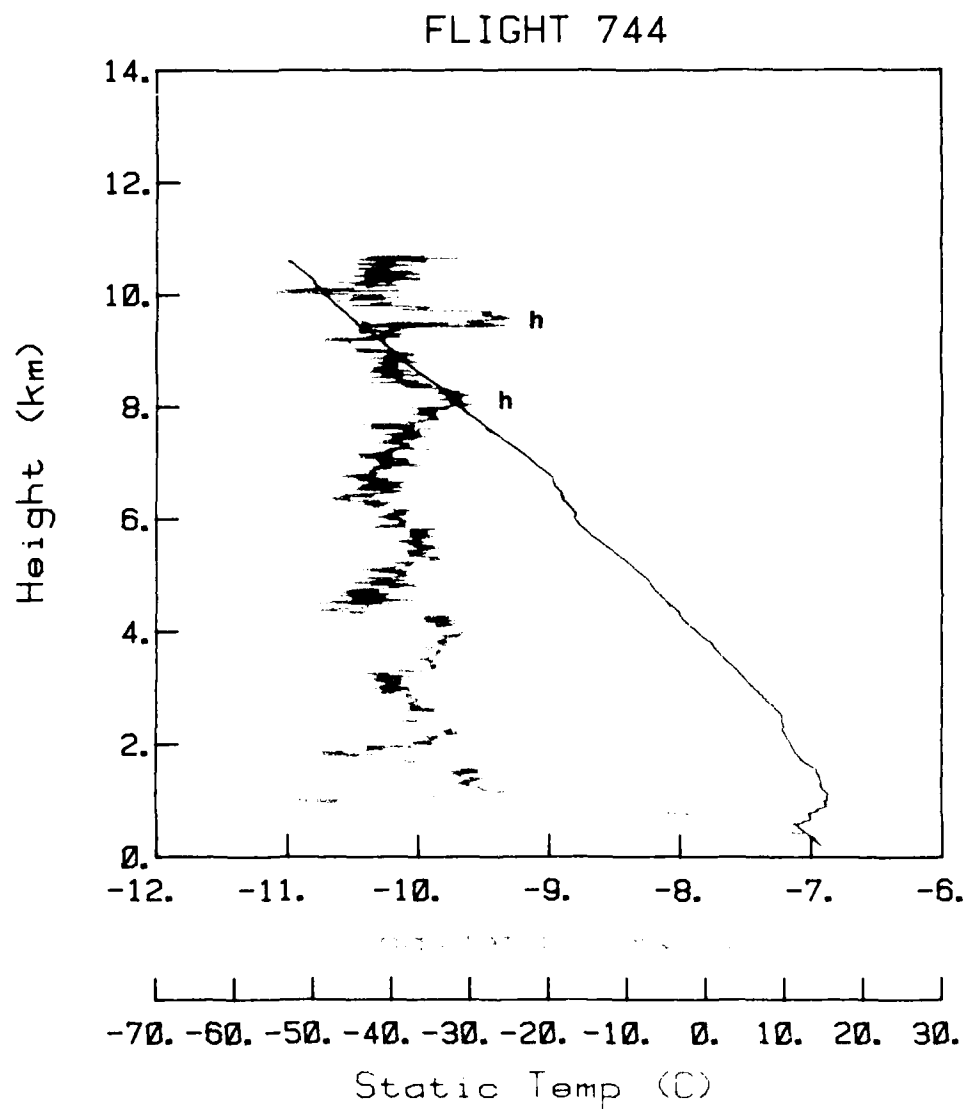


Figure 5A. Climb out of Lisbon, 7 June 1982. Observer's log records slight haze at h.

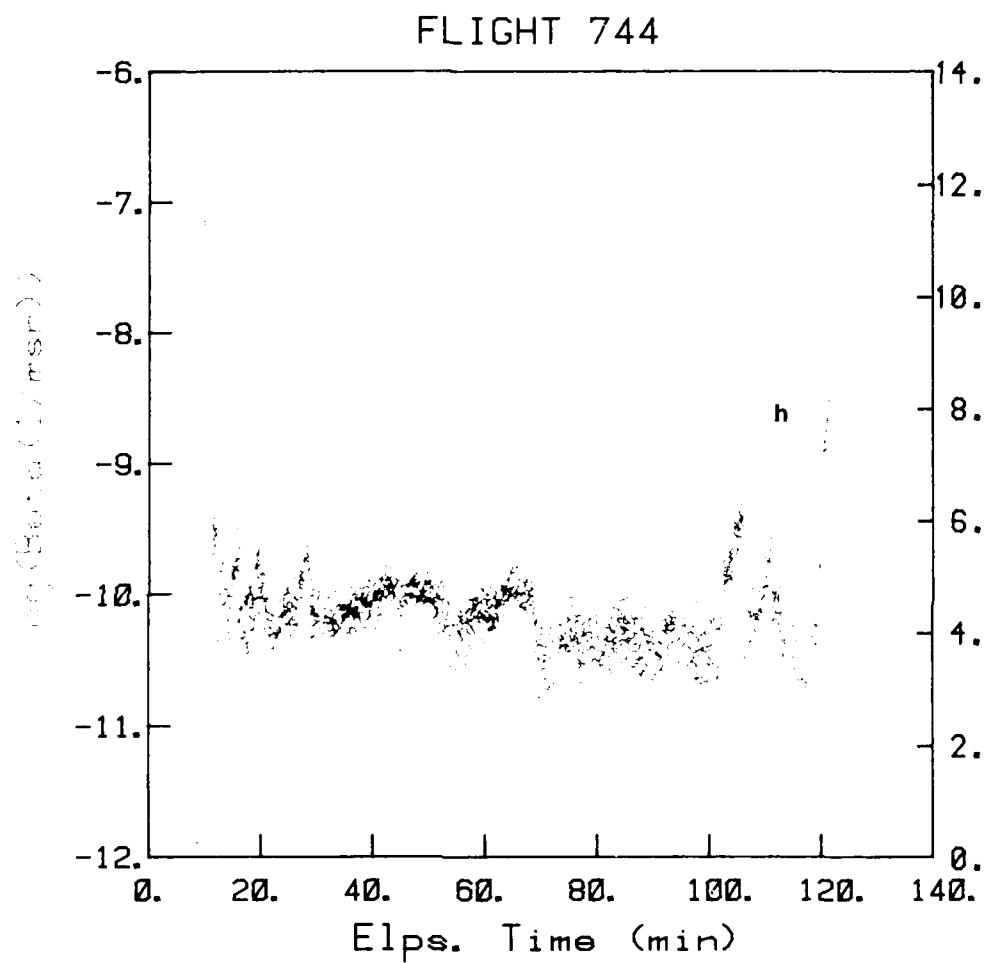


Figure 5B. Transit Lisbon-north, 7 June 1982. Observer's log records a strong haze layer on approaching the French coast at h.

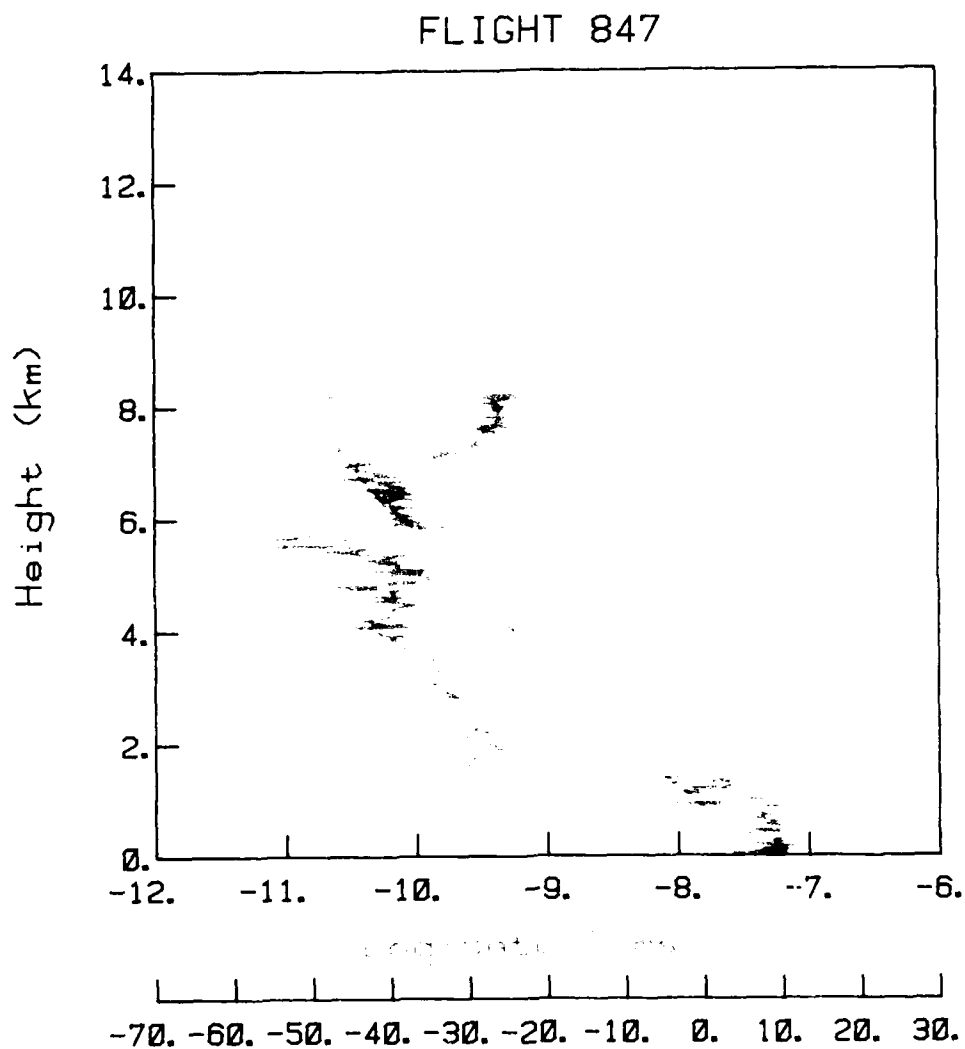


Figure 6A. Climb out of Lisbon, 9 February 1983. The occasional gaps are due to faulty recording. The observer's log records haze up to 3 km and slight haze at 8 km. Note the order of magnitude increase in $\beta(\pi)$ in the final 1 km of climb as the aircraft probably passes through the low tropopause (see also the record for Flight 850 - figure 8 - made 3 days later with similar low tropopause).

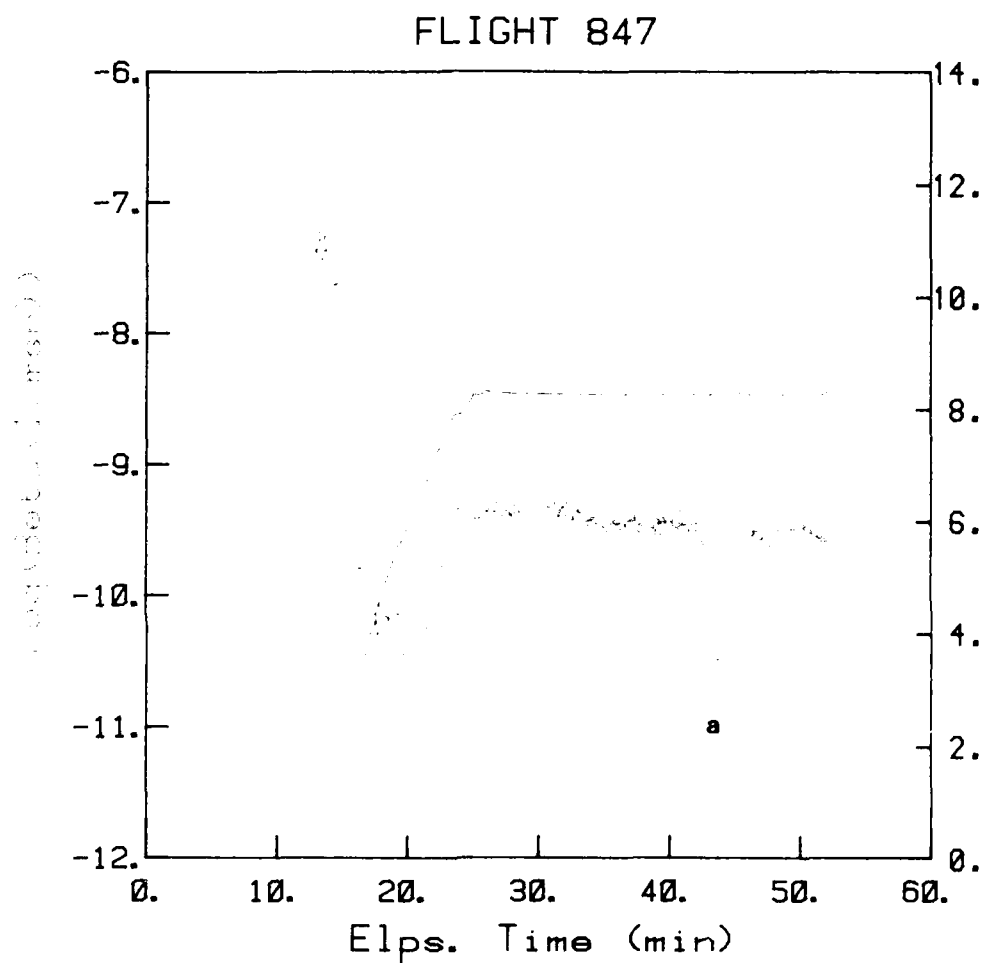


Figure 6B. Transit Lisbon-Faro-Gibraltar, 9 February 1983. Note the uniformly high level of $\beta(\pi)$ at ~ 8.4 km apart from region 'a' which is probably an intrusion of tropospheric air (although there is no strong anomaly in the temperature record that would verify this).

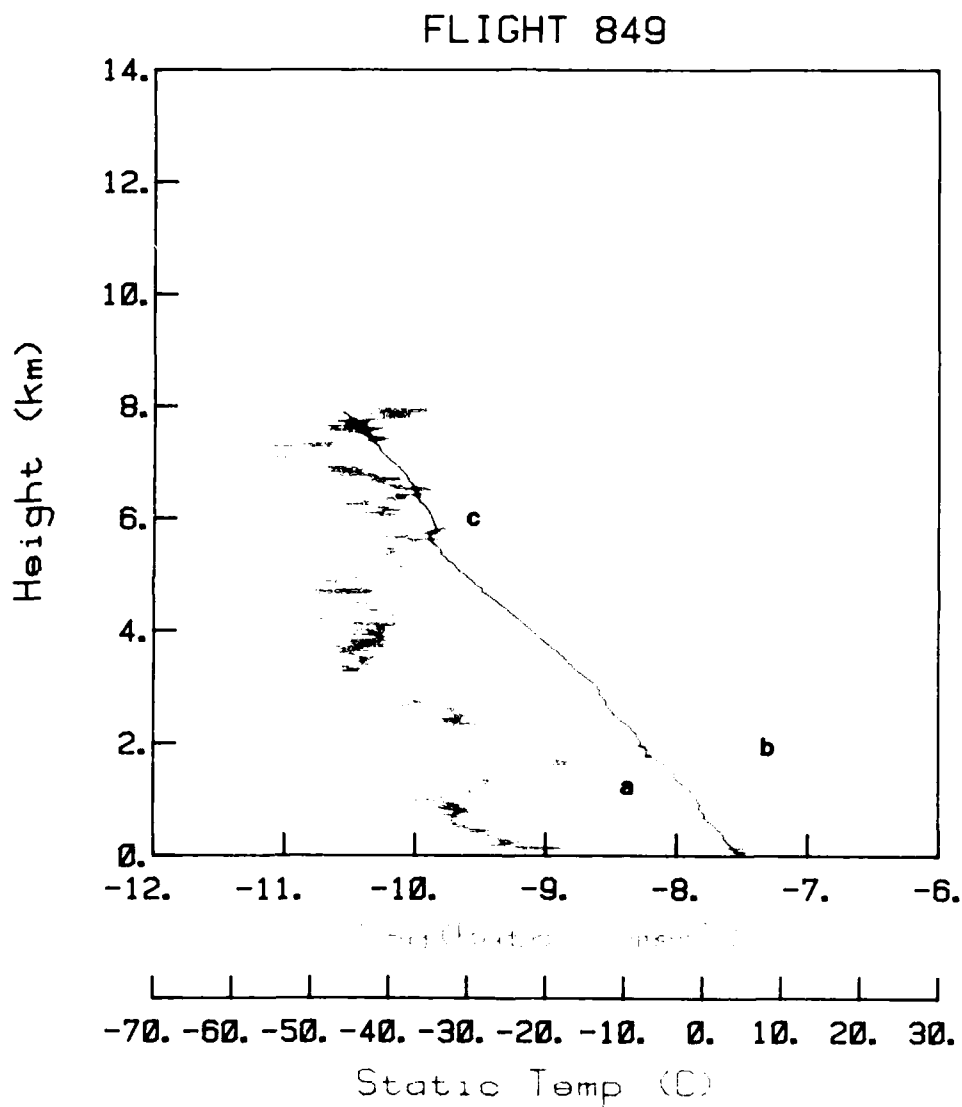


Figure 7A. Climb out of Gibraltar, 12 February 1983. Observer's log records haze at a, a thin cloud layer at b (and saturated signal). The gap at c is where the signal had fallen to a very low level over a very narrow height interval — possibly associated with the temperature inversion

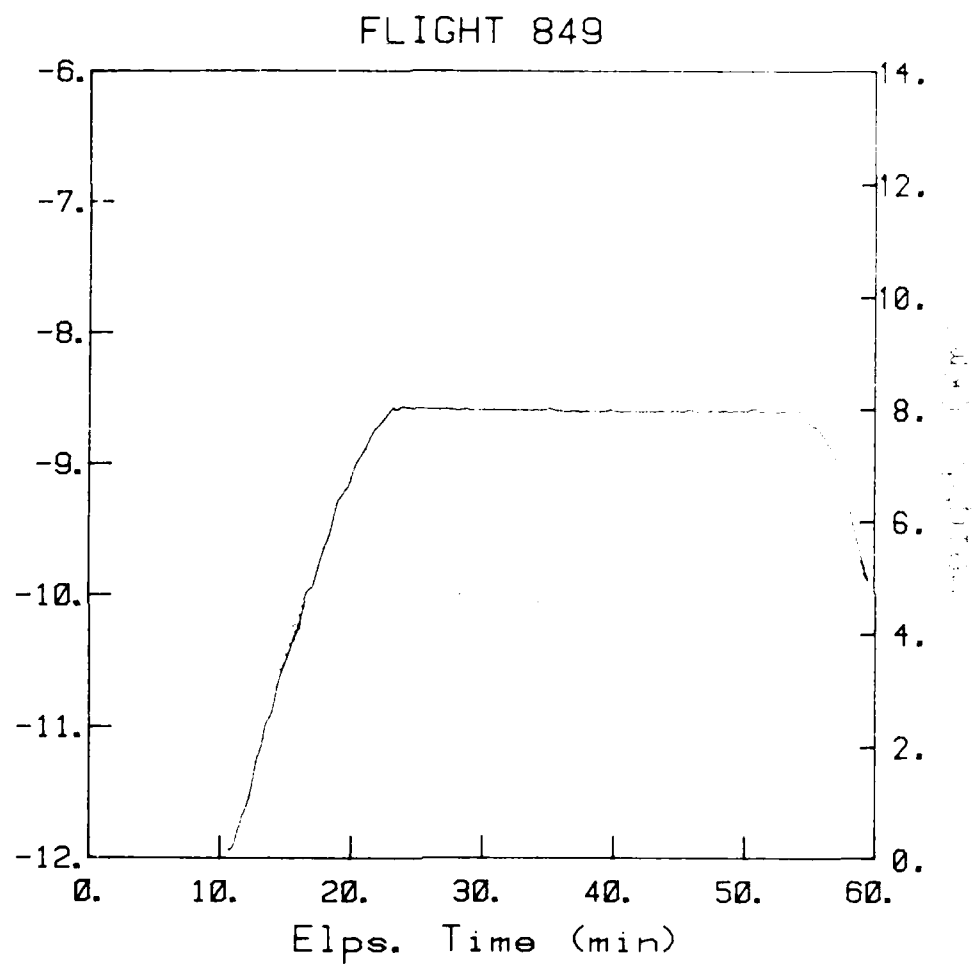


Figure 7B. Transit Gibraltar-Faro-Lisbon, 12 February 1983

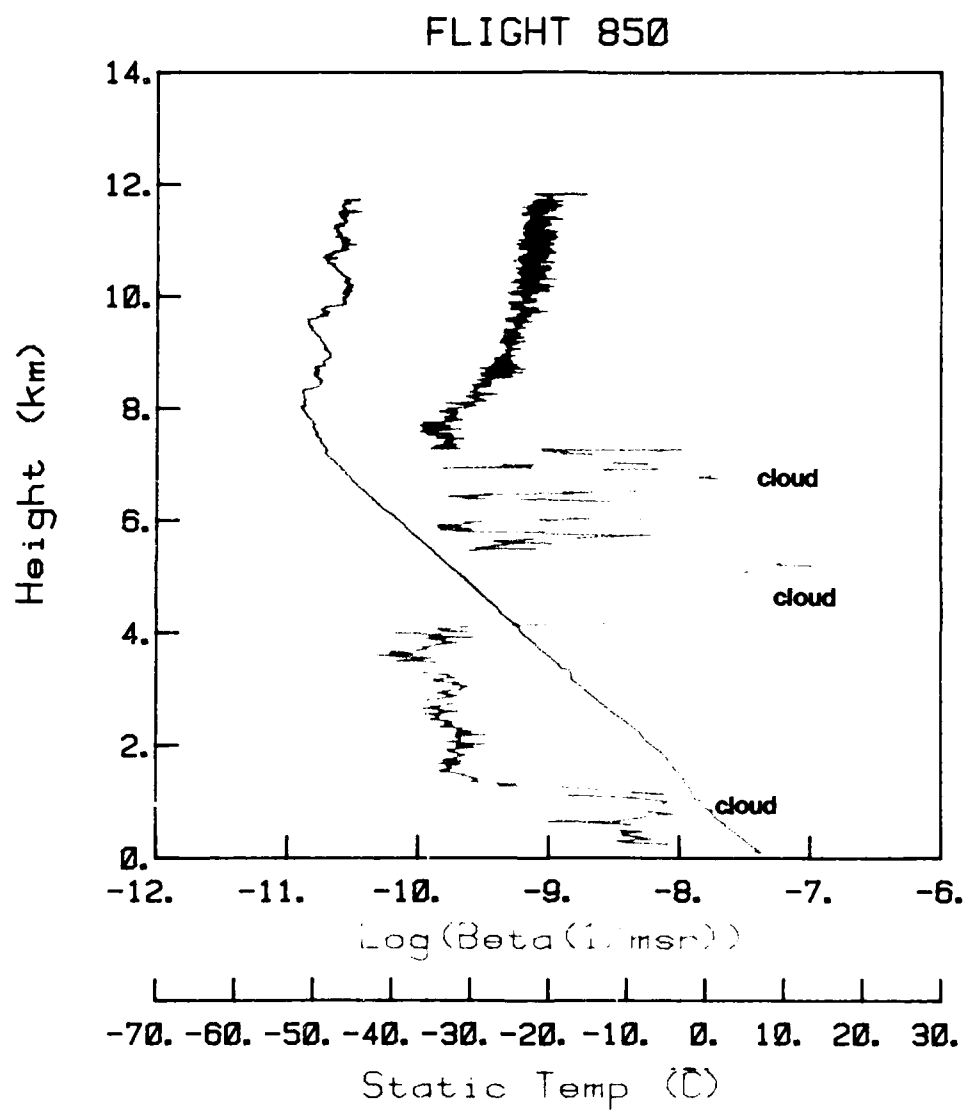


Figure 8A. Climb out of Lisbon, 12 February 1983. The observer's log records cloud at < 1 km and in and out of cloud at 4-7 km, with clear air above. Note the steady increase in $\beta(\pi)$ as the aircraft climbs above the low tropopause and into the stratosphere from ~ 8 km.

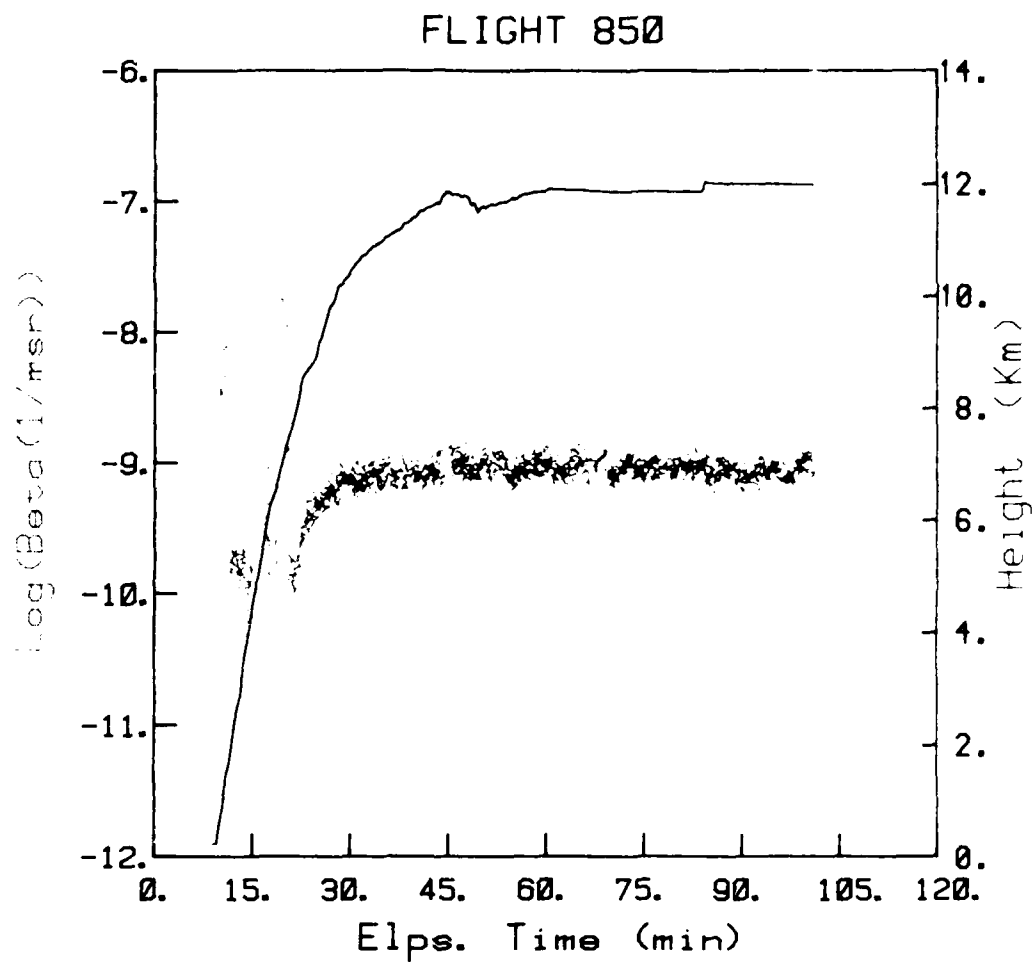


Figure 8B. Transit Lisbon-north, 12 February 1983. From 45 minutes onwards there is some suggestion of a small cyclic variation in the backscatter level with ~ 5 minute period. (This is more obvious on an extended timescale). Overall, however, the level of $\beta(\pi)$ remains remarkably constant at a high value just below $\sim 10^{-9} \text{ m}^{-1} \text{ sr}^{-1}$ for ~ 70 minutes flying time.

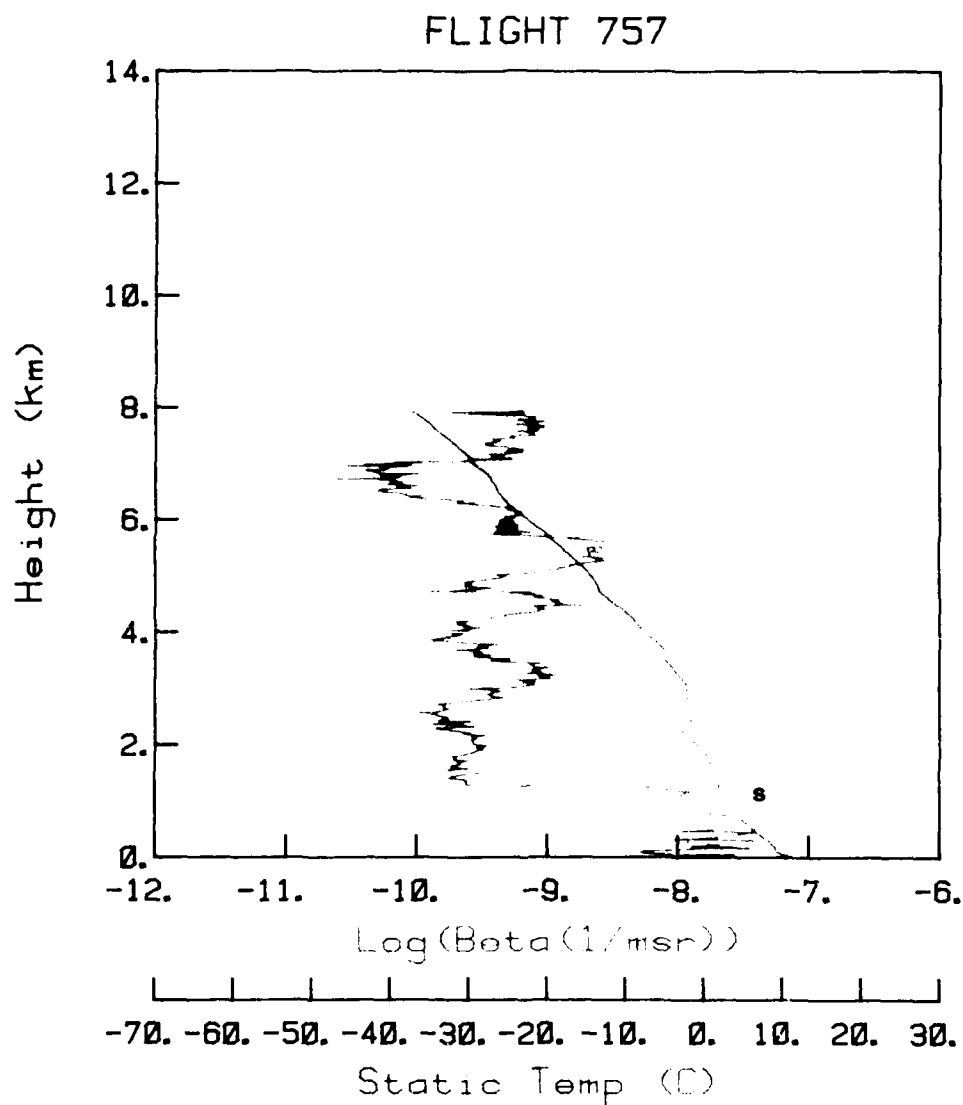


Figure 9A. Climb out of Keflavik, 22 June 1982. Observer's log records slight haze during the climb, thickest at 5.5 km. Region s had very strong scattering and signal saturation. Note the reduction in $\beta(\pi)$ of at least two decades above the inversion at ~ 1.2 km.

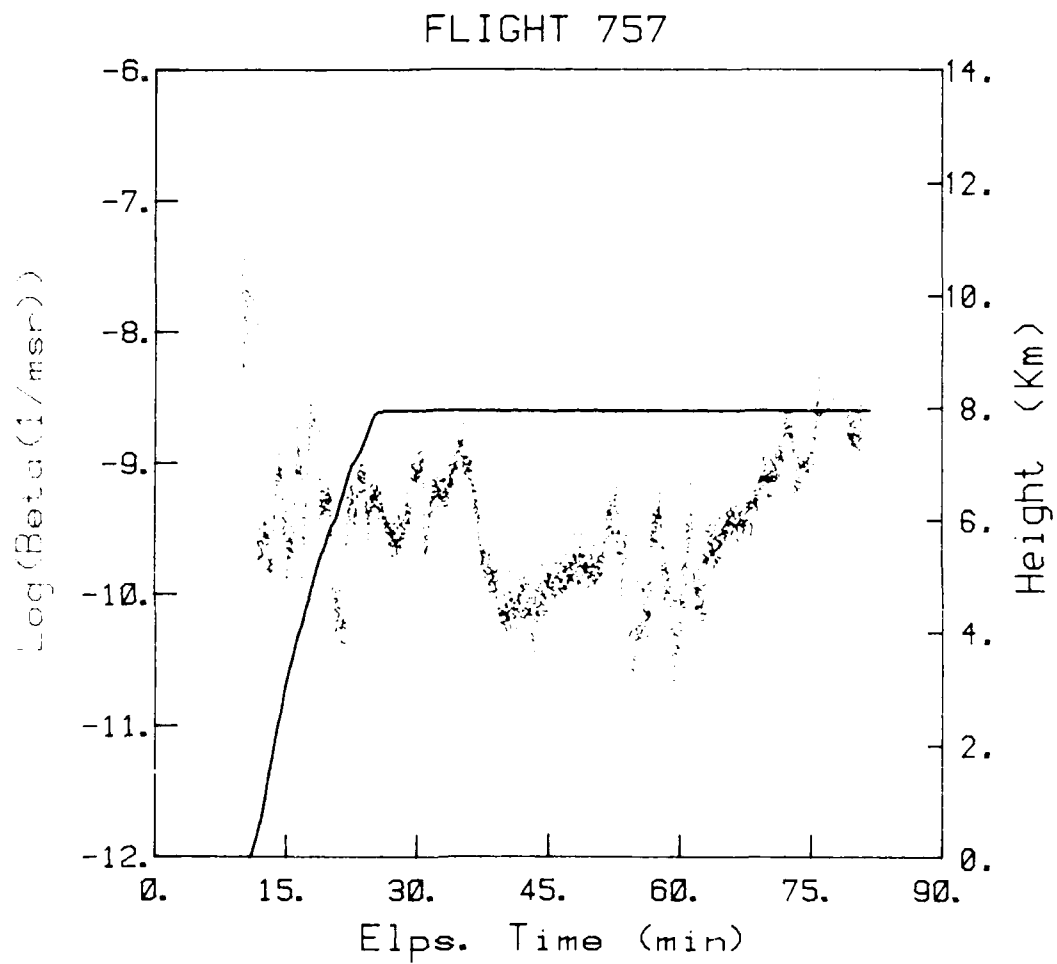


Figure 9B. Keflavik-Sondre Stromfjord, 22 June 1982. The log records thicker haze approaching the coast of Greenland (from 75 minutes).

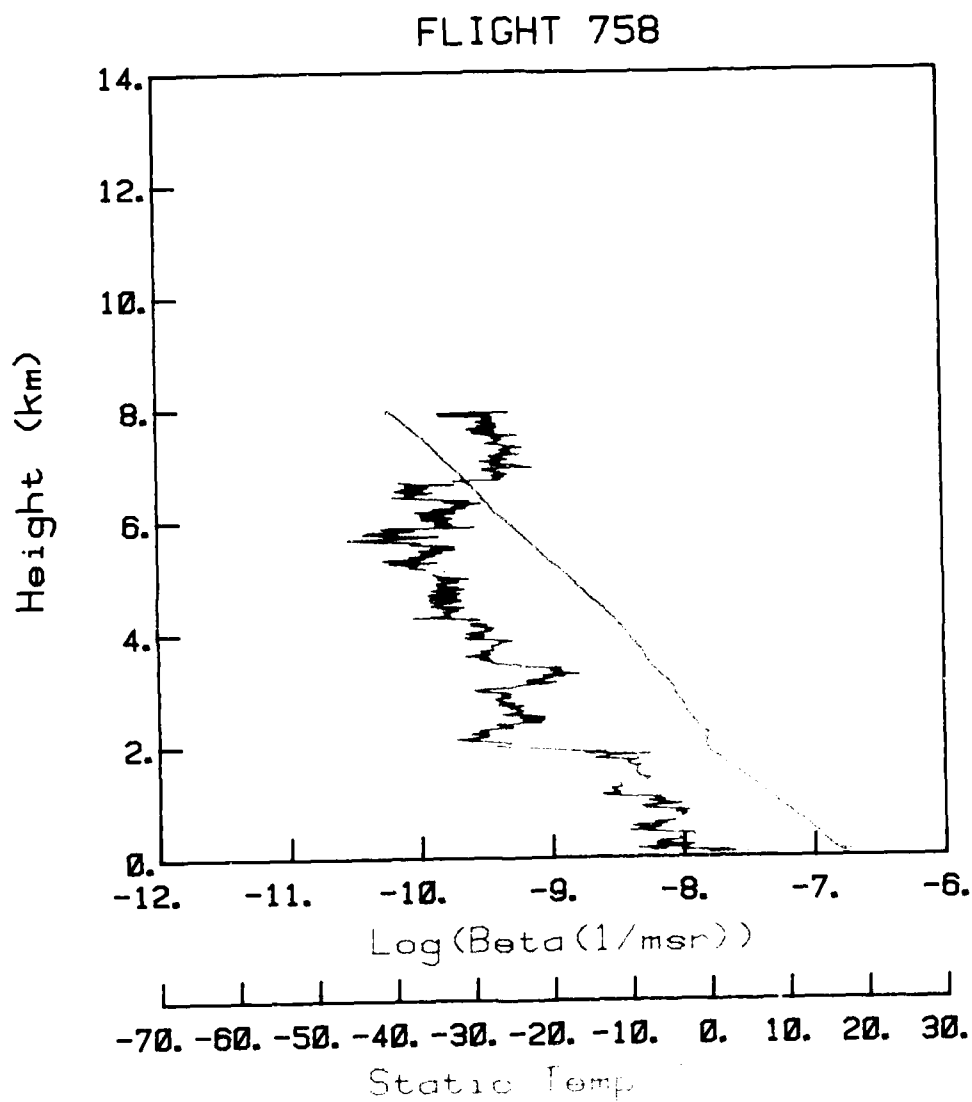


Figure 10A. Climb out of Sondre Stromfjord, 22 June 1982.

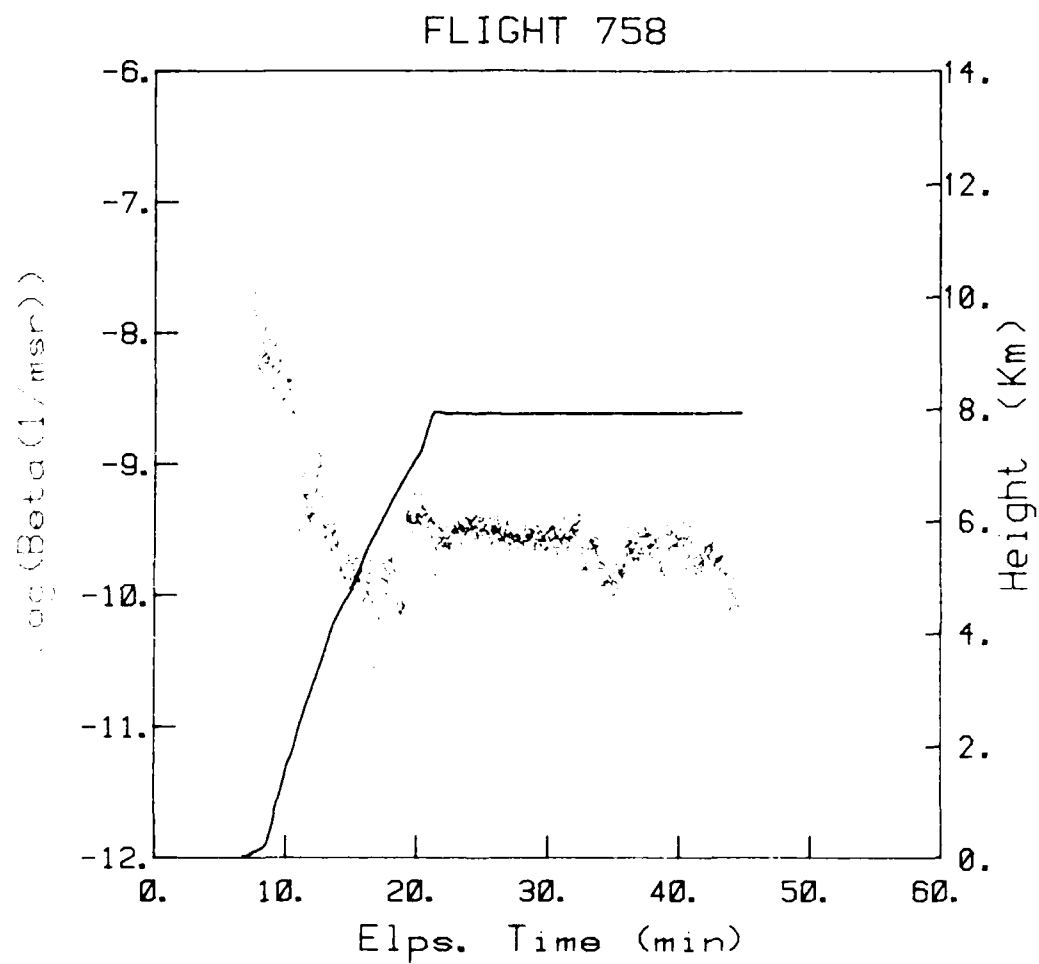


Figure 10B. Sondre Stromfjord-Keflavik, 22 June 1982.

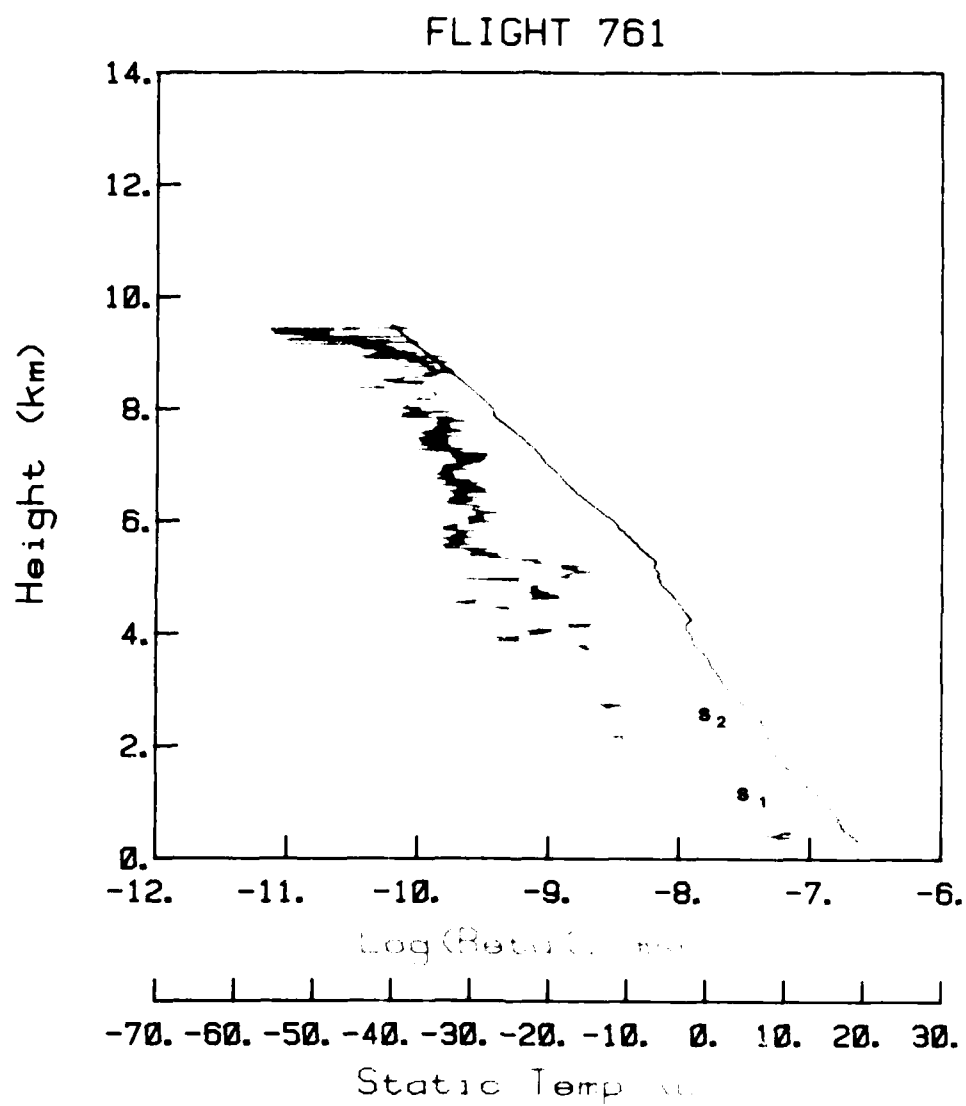


Figure 11A. Climb out of Chicago (O'Hare), 24 June 1982. Haze to 5 km was recorded. The signal was strongly saturated in regions s_1 and s_2 .

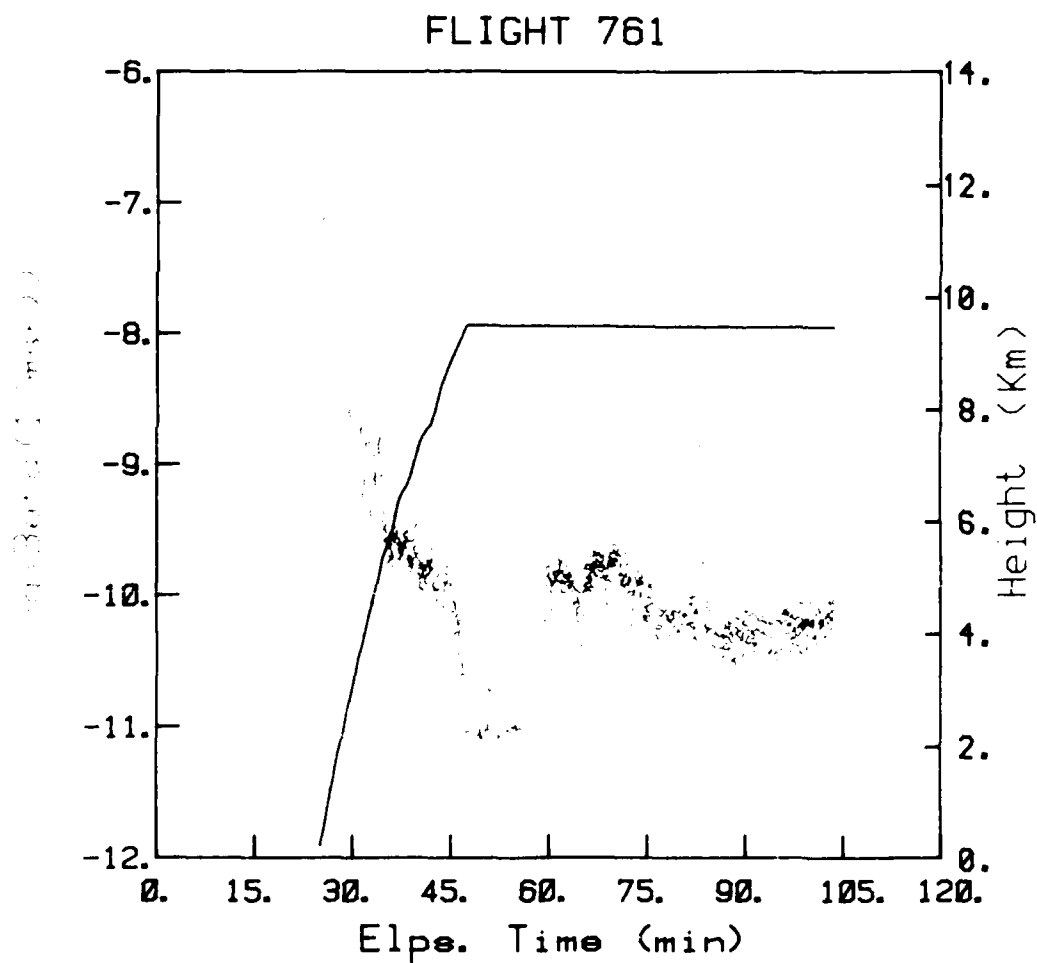


Figure 11B. Chicago-Denver, 24 June 1982. The low signal at 47-59 min with apparent bimodal distribution is discussed further in the text and figures 28 and 29. This one of the few continuous stretches (~ 100 km) of consistently low signal with $\beta(\pi)$ at or below $\sim 4 \times 10^{-11} \text{ m}^{-1} \text{ sr}^{-1}$.

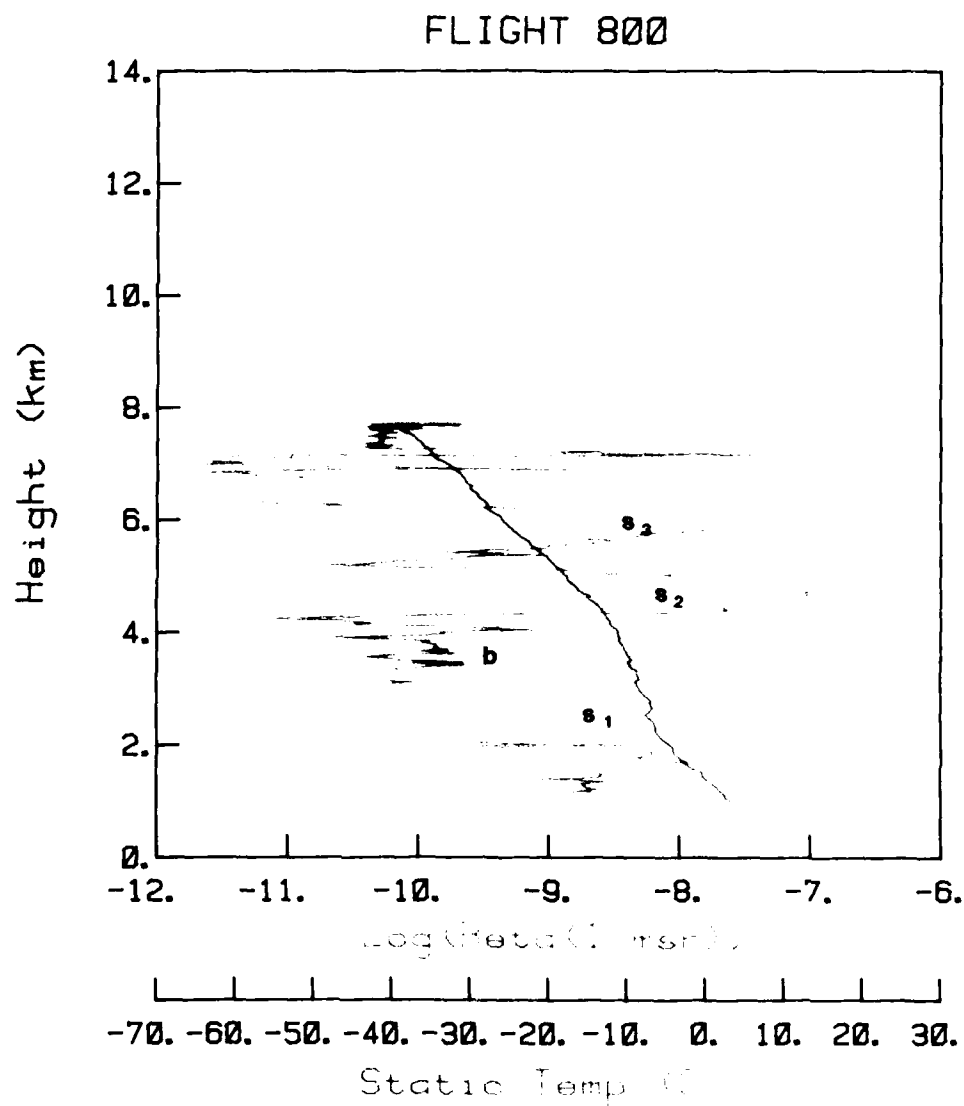


Figure 12A. Climb out of Frobisher, 19 June 1982. Observer's log: region s_1 - in cloud, saturated signal; region b - clear above cloud; region s_2 - thick haze, signal saturating; region s_3 - haze.

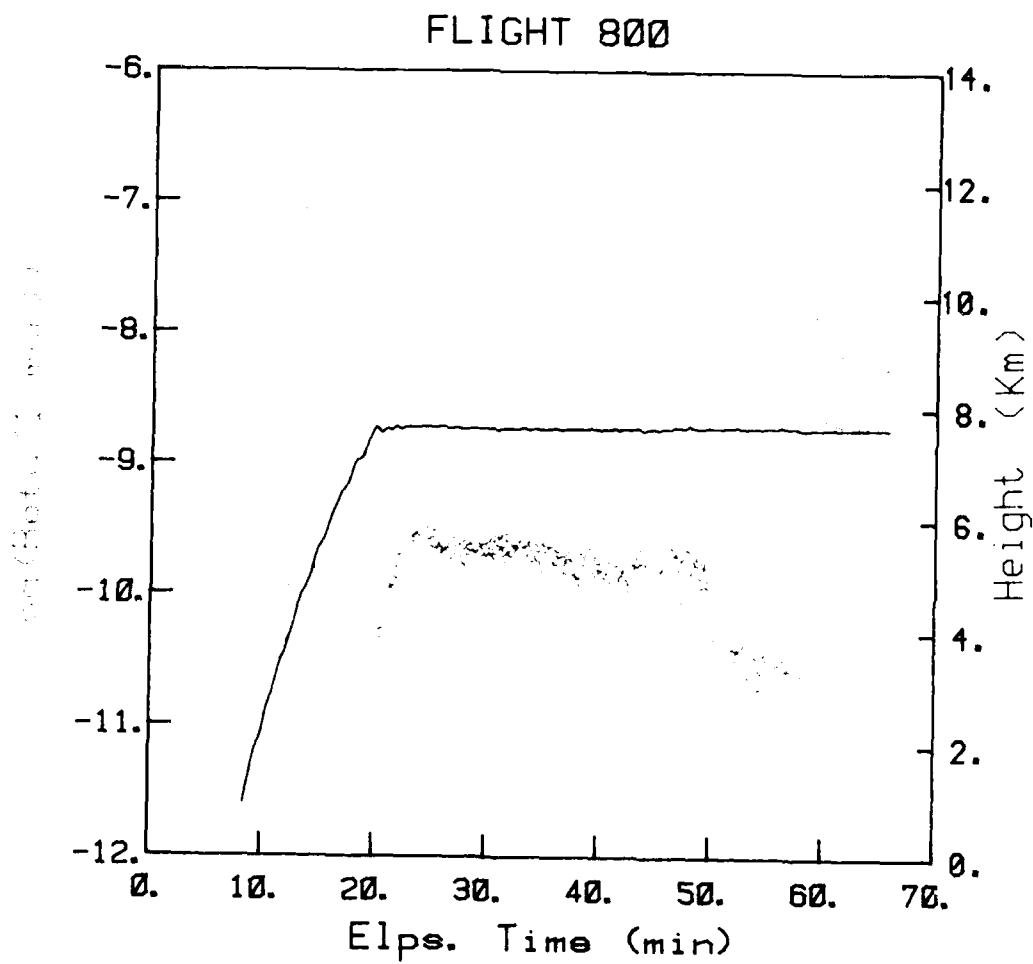


Figure 12B. Frobisher-Sonde Stromfjord, 19 July 1982. Note the haze layers during the climb. Observer's log records turbulence at 37 min (possibly in jet stream); in calmer air later and cloud at end.

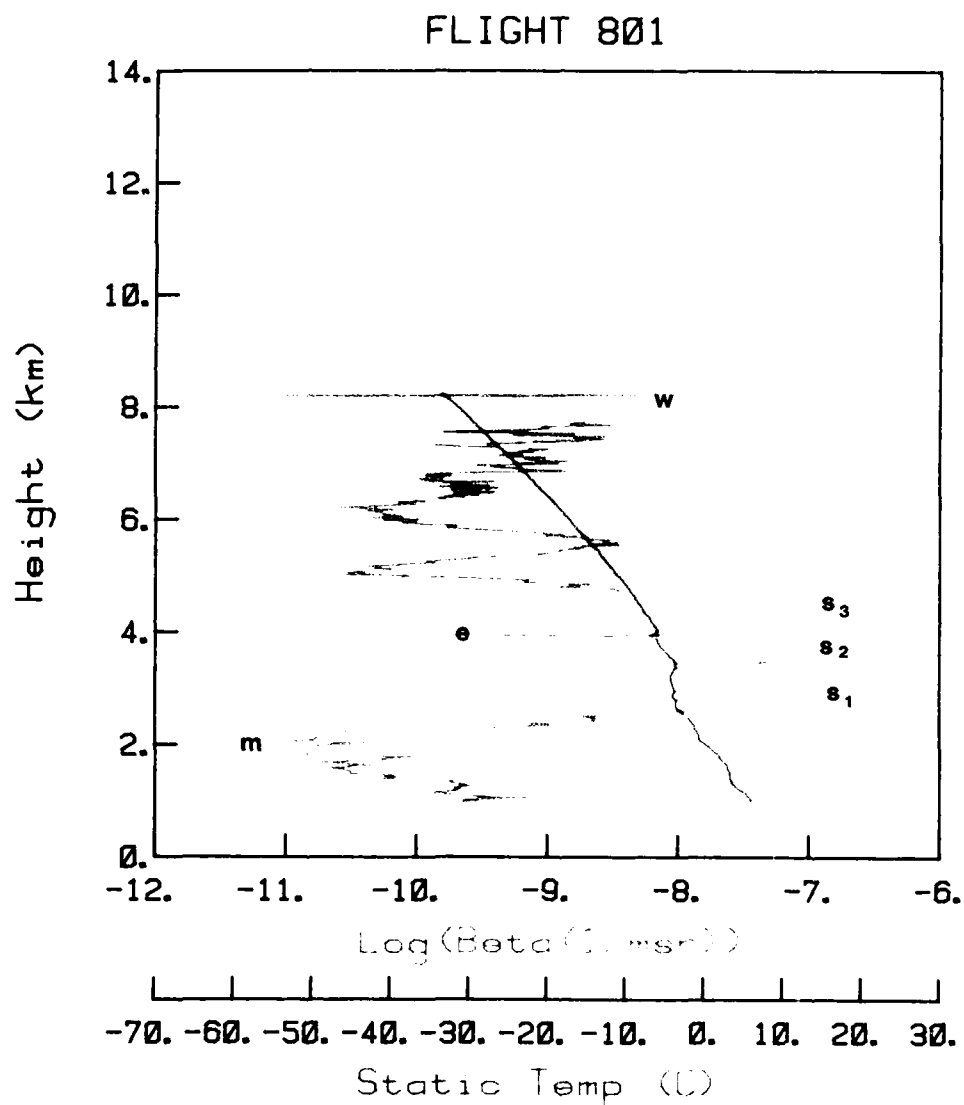


Figure 13A. Climb out of Sondre Stromfjord, 19 July 1982. Observer's log: m - signal falling to minimum detectable at 2 km; s₁, s₂, s₃ - cloud layers and saturating signals; e - period of level flight at 4 km, part in cloud; w - sudden 'complete whiteout' in Arctic haze - saturated signal.

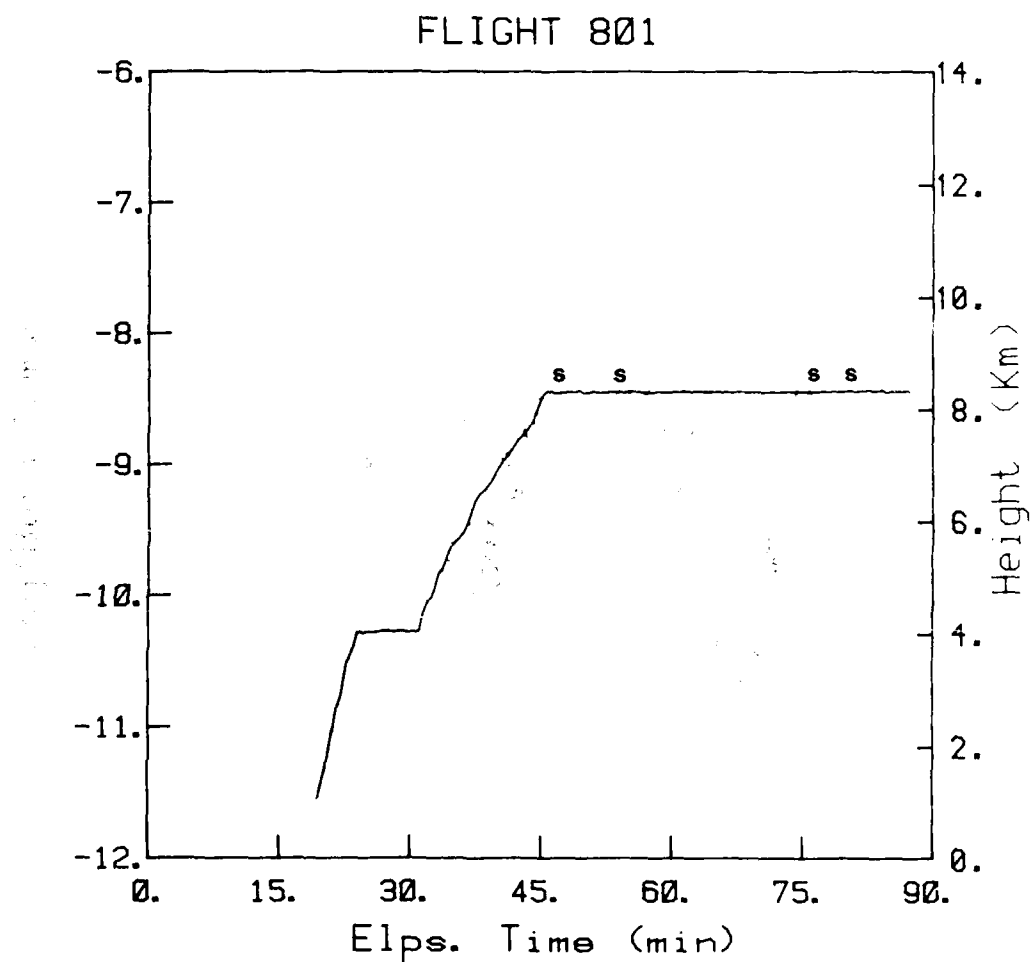


Figure 13B. Sondre Stromfjord-Keflavik, 19 July 1982. Intermittent cloud and haze and for the regions marked s the data shows saturating signals. Number of integrations: 4×10^3 .

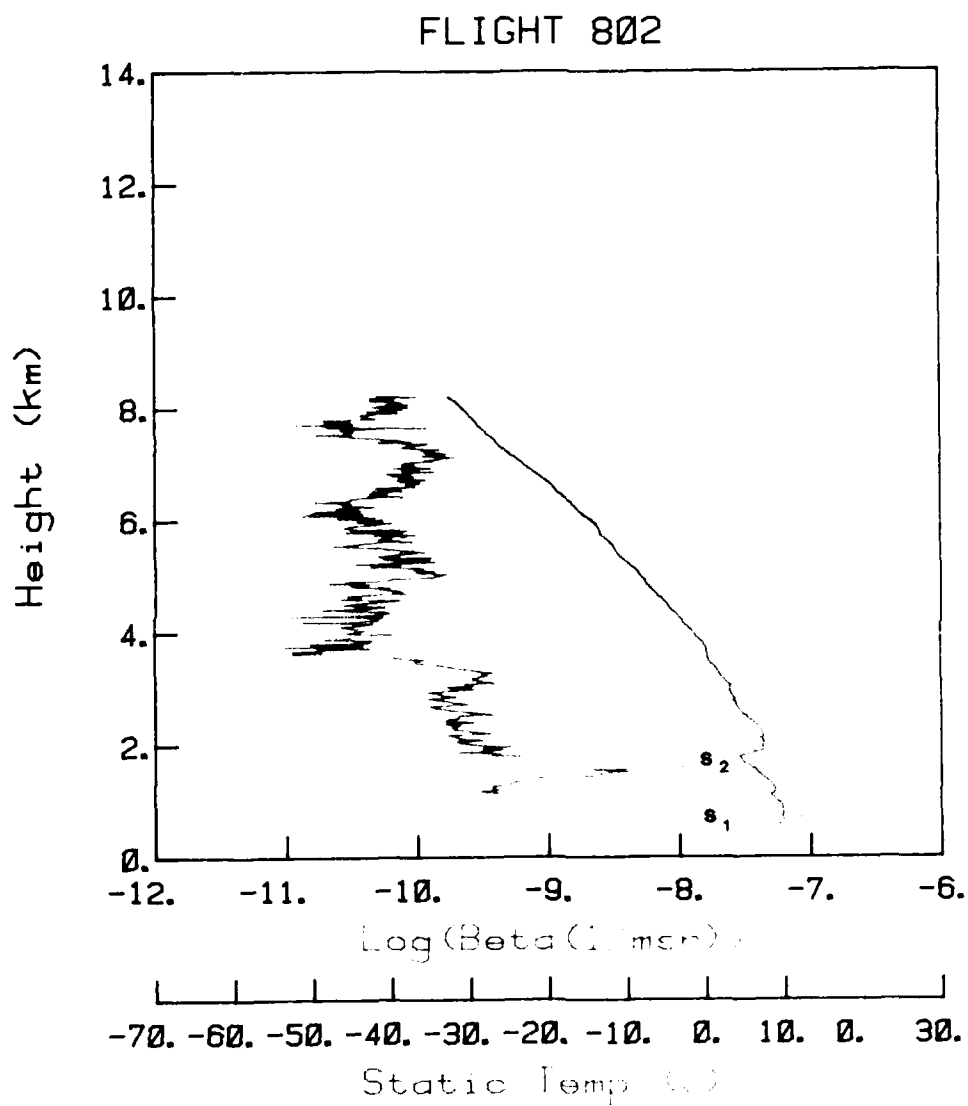


Figure 14A. Climb out of Keflavik, 20 July 1982. The log records some cloud and haze at low level and the data shows signal saturation at the regions marked s_1 and s_2 .

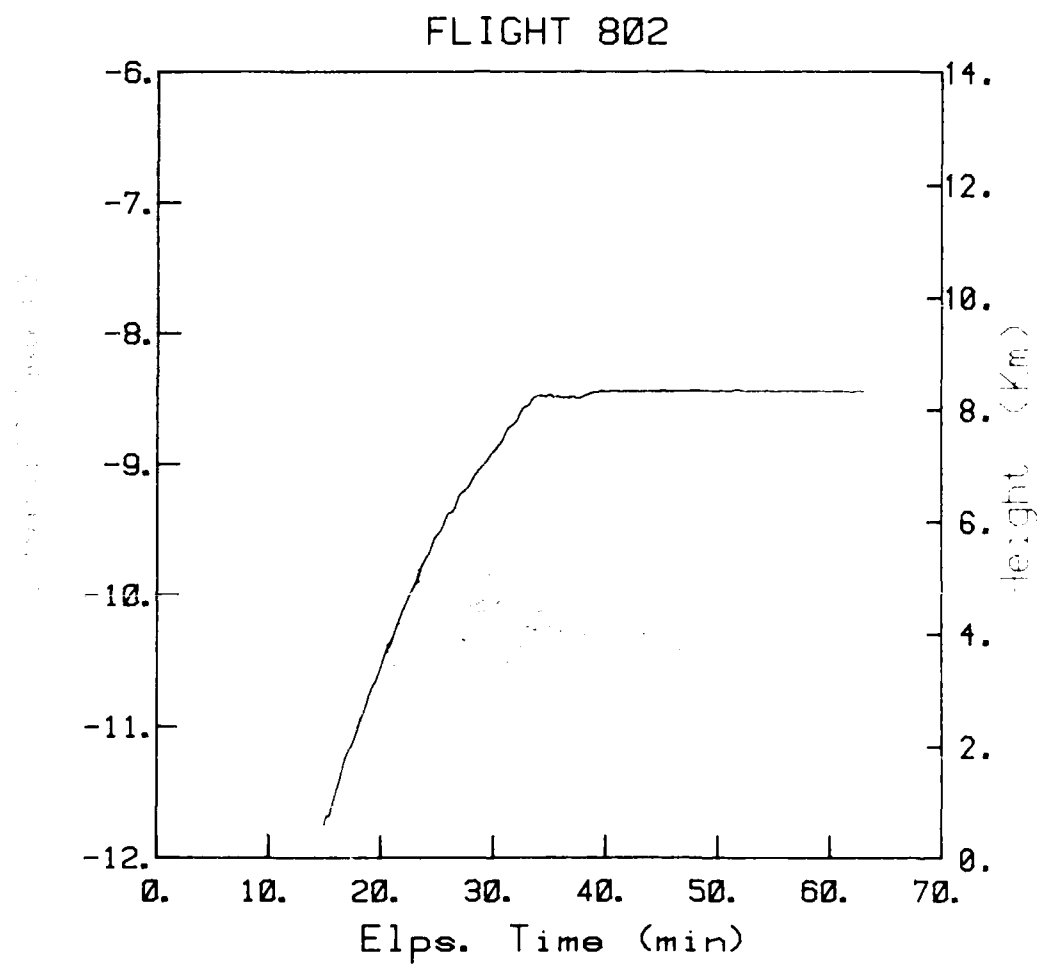


Figure 14B. Keflavik-Lossiemouth, 20 July 1982. Note the strong variation in backscatter level during the transit. Number of integrations: 4×10^3 .

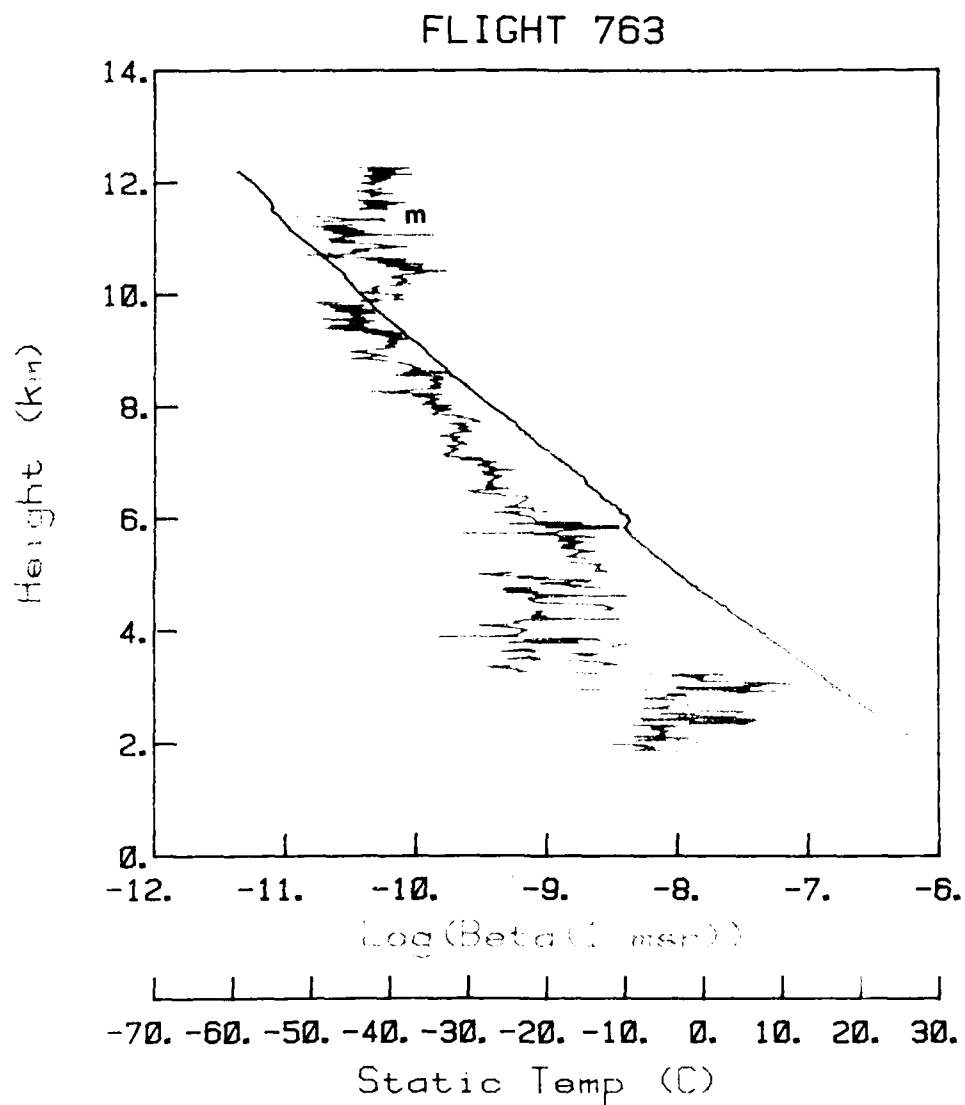


Figure 15A. Climb out of Jeffco, 28 June 1982. The log records signal lost (below minimum detectable) at ~ 11.5 km over a narrow height interval (m).

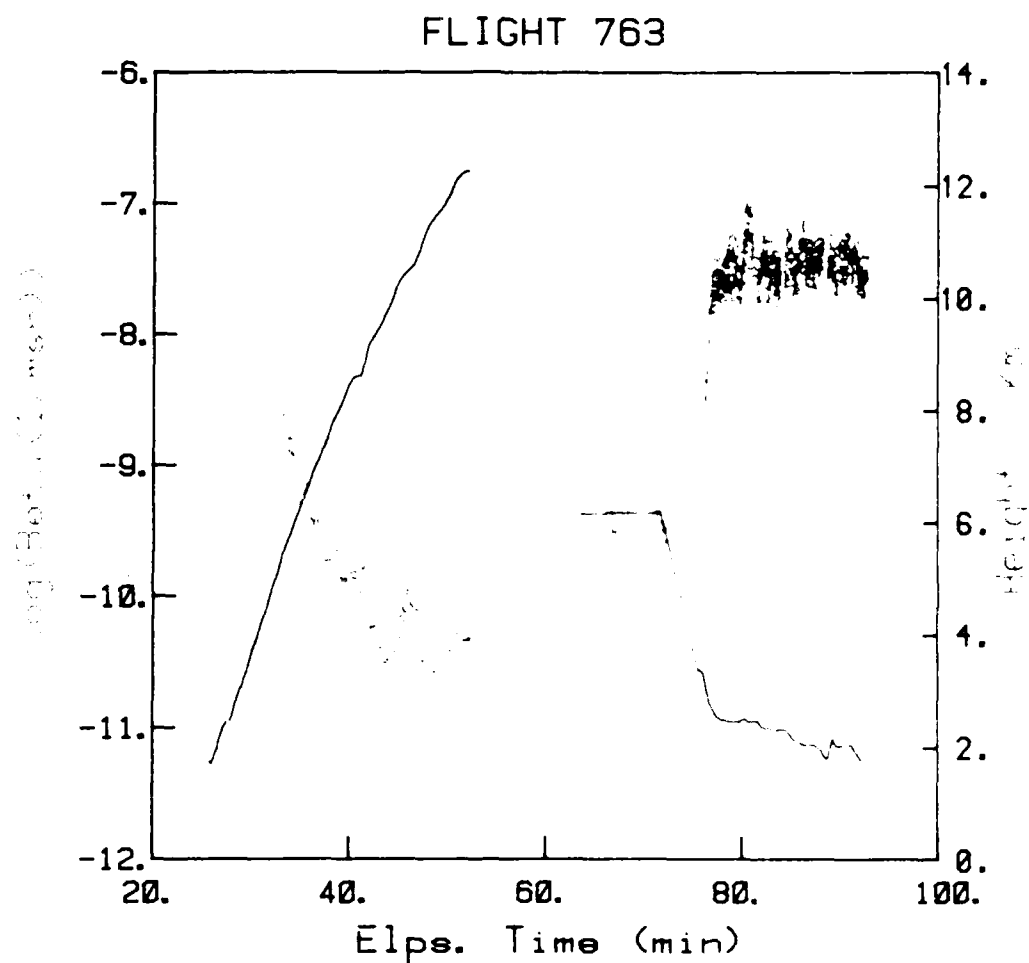


Figure 15B. Flight out of Jeffco, 28 June 1982. The only data recorded during this first trial flight in Colorado was the climb, a few short intermittent runs at ~ 6 km and a longer run at low altitude (3 to 2 km) where the signal was very strong (and often saturated)

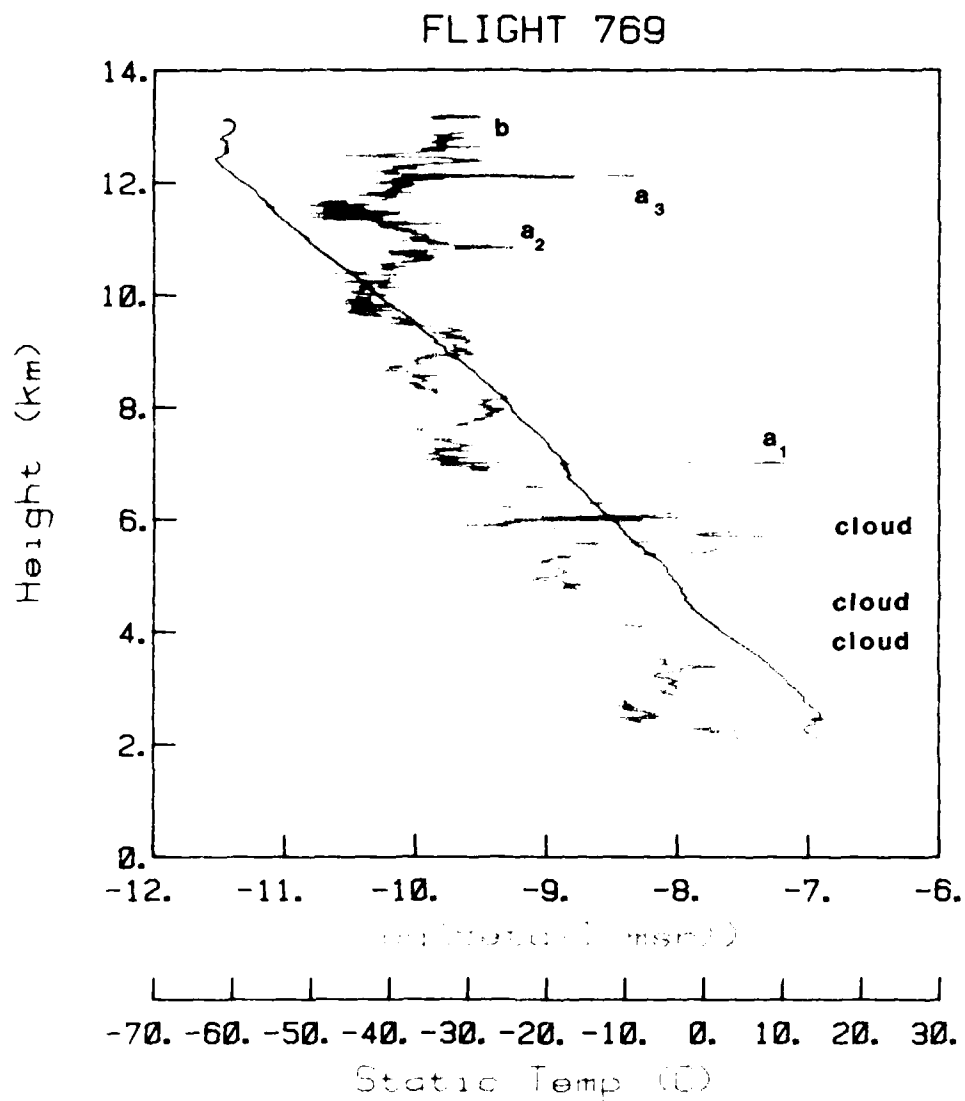


Figure 16A Climb out of Jeffco, 1 July 1982, heading 015° for about 240 km. There was intermittent cloud to about 6 km altitude giving rise to gaps in the record due to saturation. The strong peaks at a were initially thought to be spurious but were also found on descent over similar very narrow height intervals. From the ascent rate these intervals are, at most, only a few tens of metres deep. At b the spectral peak was too close to the end of the spectrum and could not be processed — hence the gap in the record.

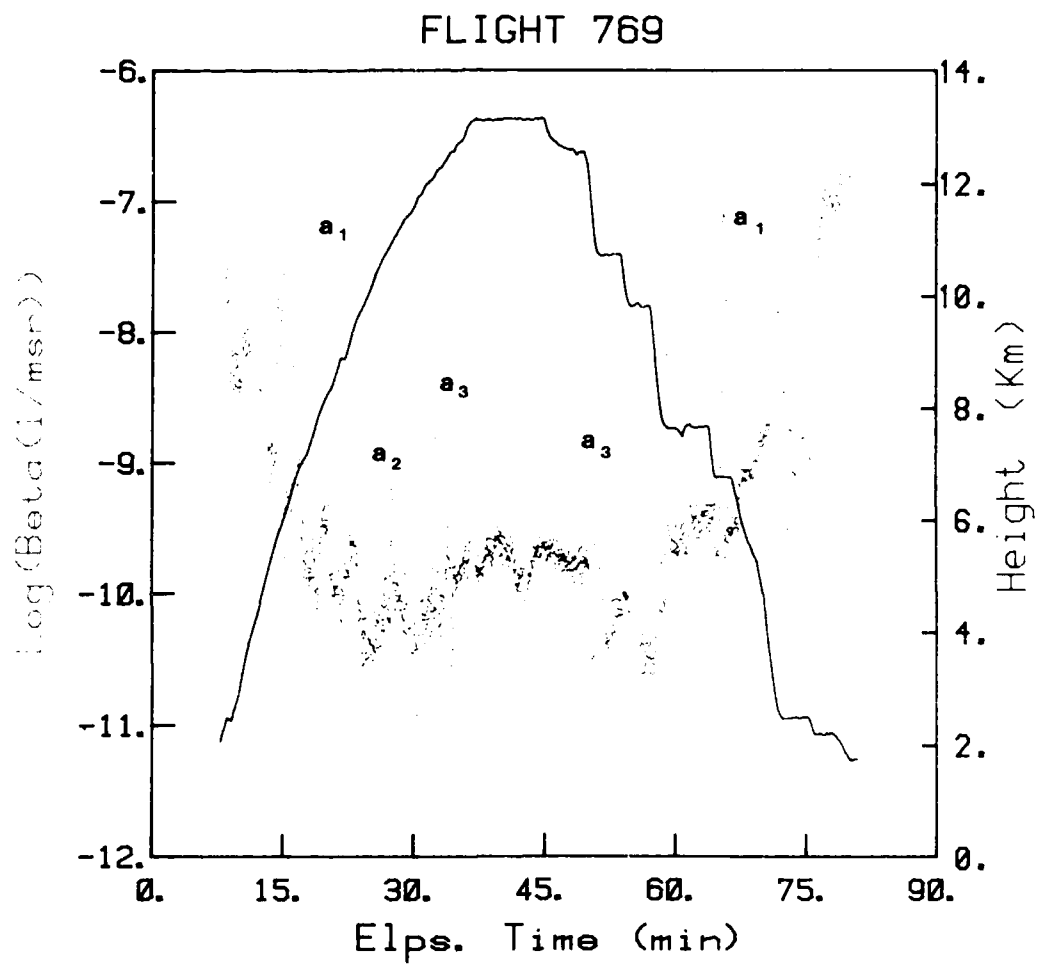


Figure 16B. Climb and return to Jeffco, 1 July 1982. The corresponding strong signals at narrow height intervals are indicated by a_1 , a_2 , a_3 . The few orbits at 13 km were flown just south of Scotts Bluff.

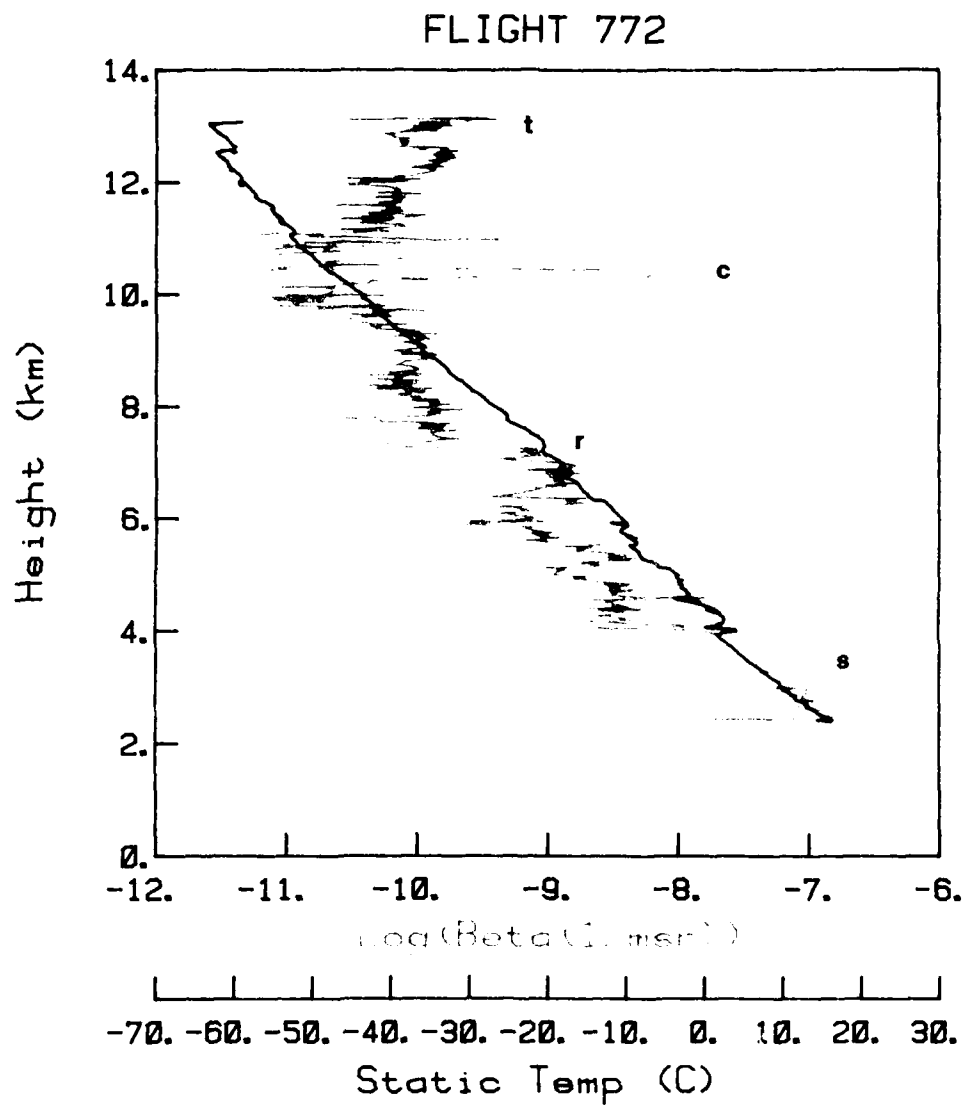


Figure 17A. Climb above Jeffco, 2 July 1982. There was strong and saturating signal from 3-4 km. The log records a sharp reduction in signal at ~ 7.1 km (r) and a thin cirrus layer on ascent at c. There was a thin haze apparent at ~ 12.5 km and some turbulence (t) at maximum altitude — possibly just into a jet stream.

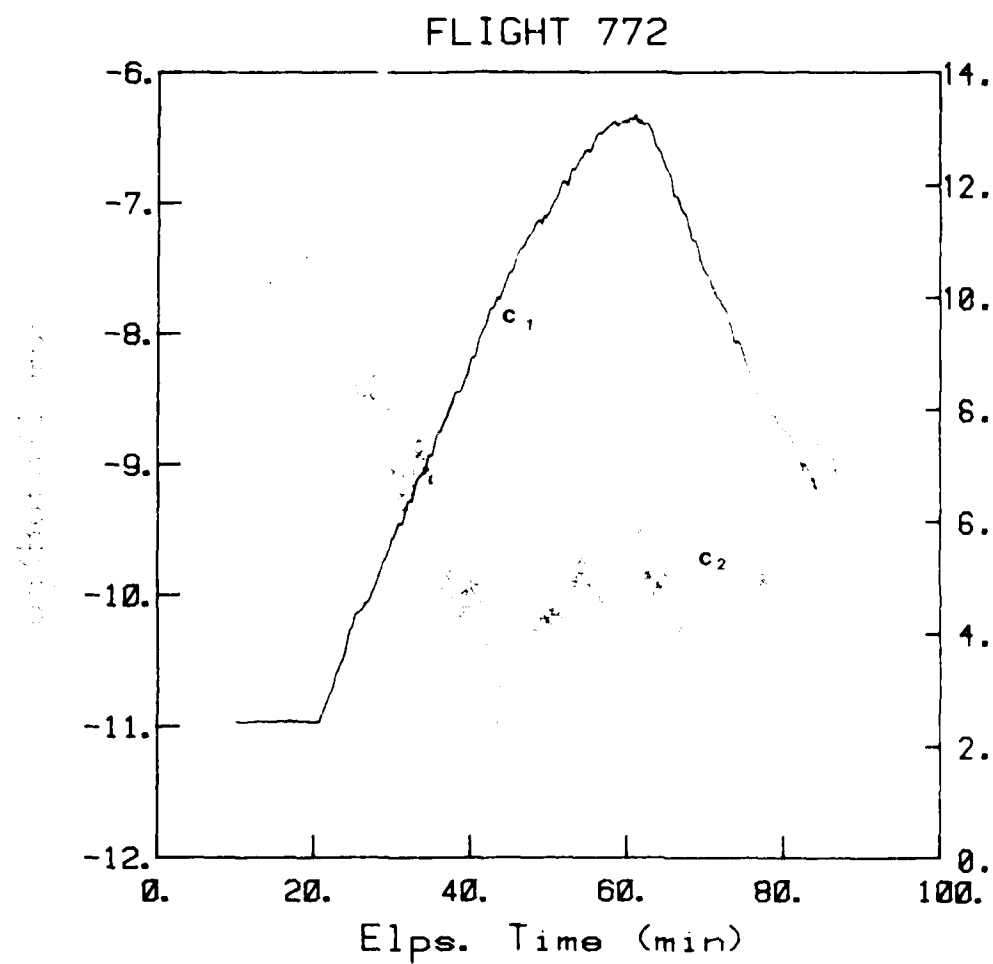


Figure 17B. Climb and descent above Jeffco, 2 July 1982. The thin cirrus layer (c_1) was not so strong on descent (c_2).

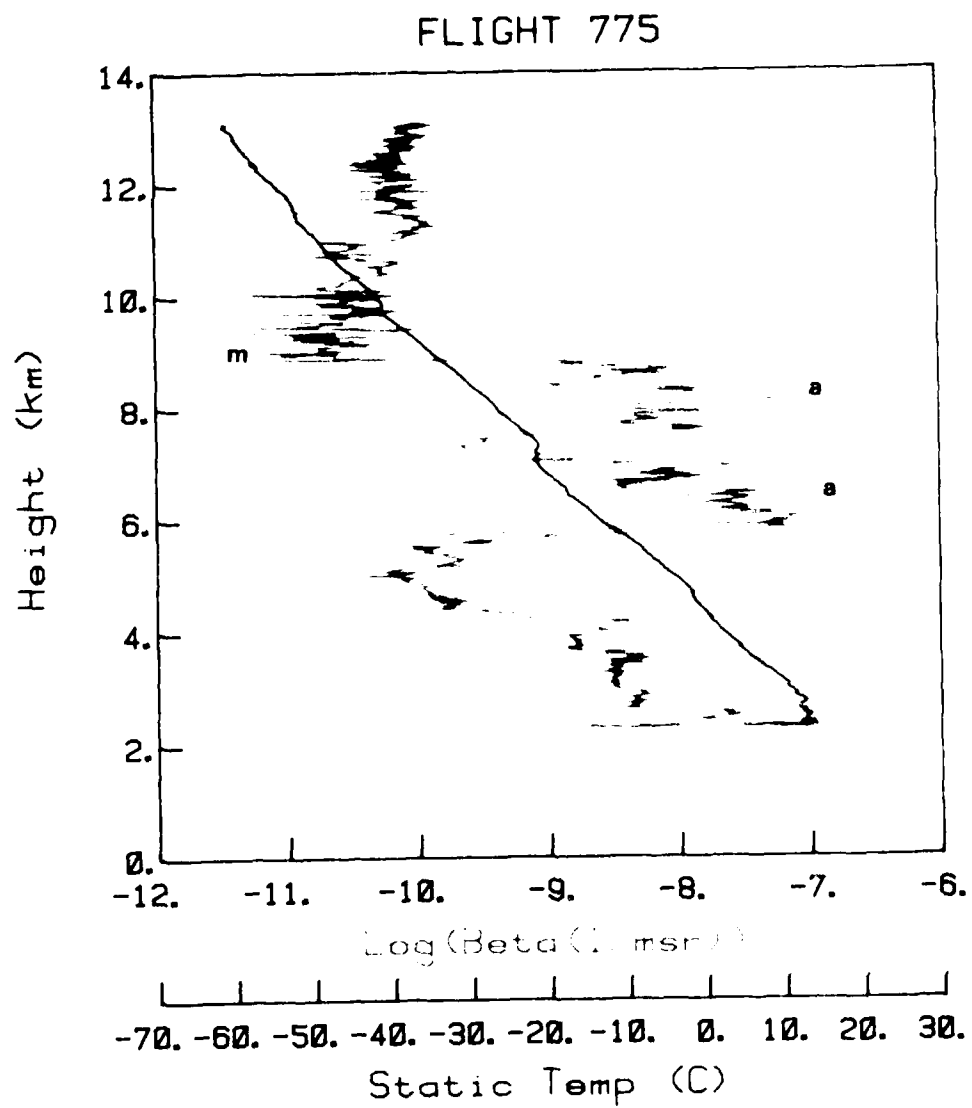


Figure 18A. Climb above Jeffco, 7 July 1982. The log records very strong signal (and some saturation) in regions a_1 , a_2 and signal at minimum detectable level at m .

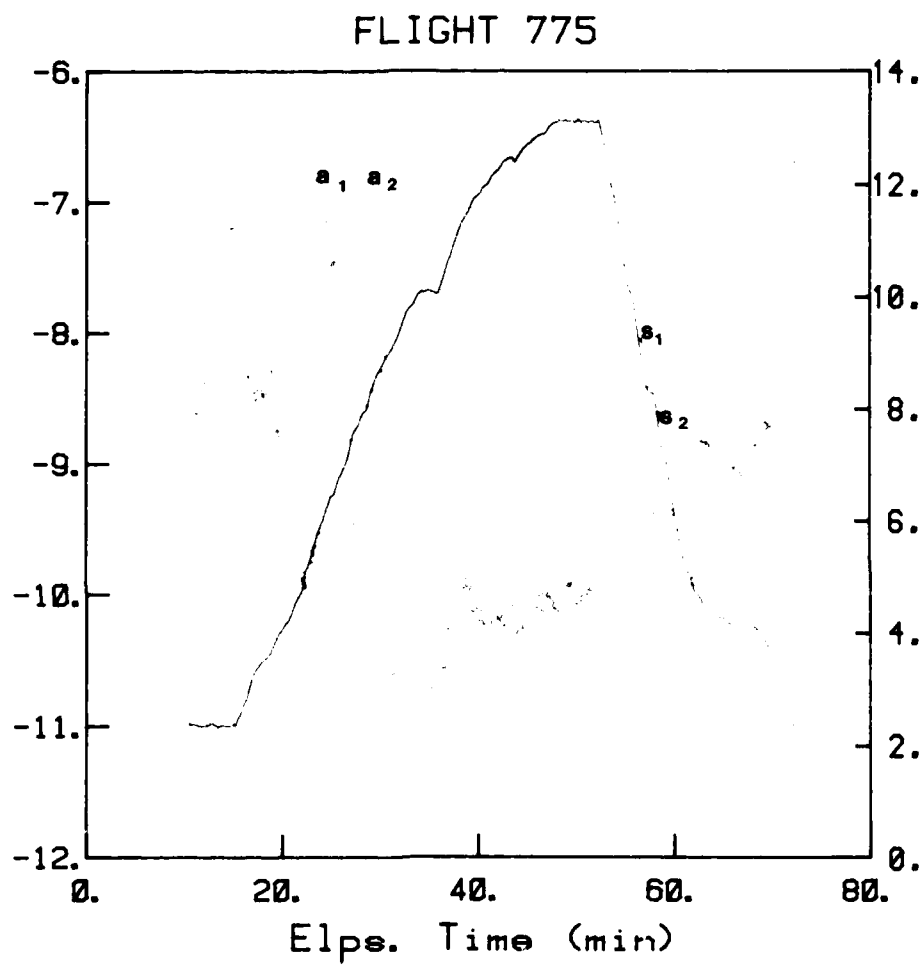


Figure 18B. Climb and rapid descent above Jeffco, 7 July 1982. The data shows saturation signals (which are not plotted) at s_1 , s_2 corresponding to the regions of strong signal on ascent a_1 , a_2 .

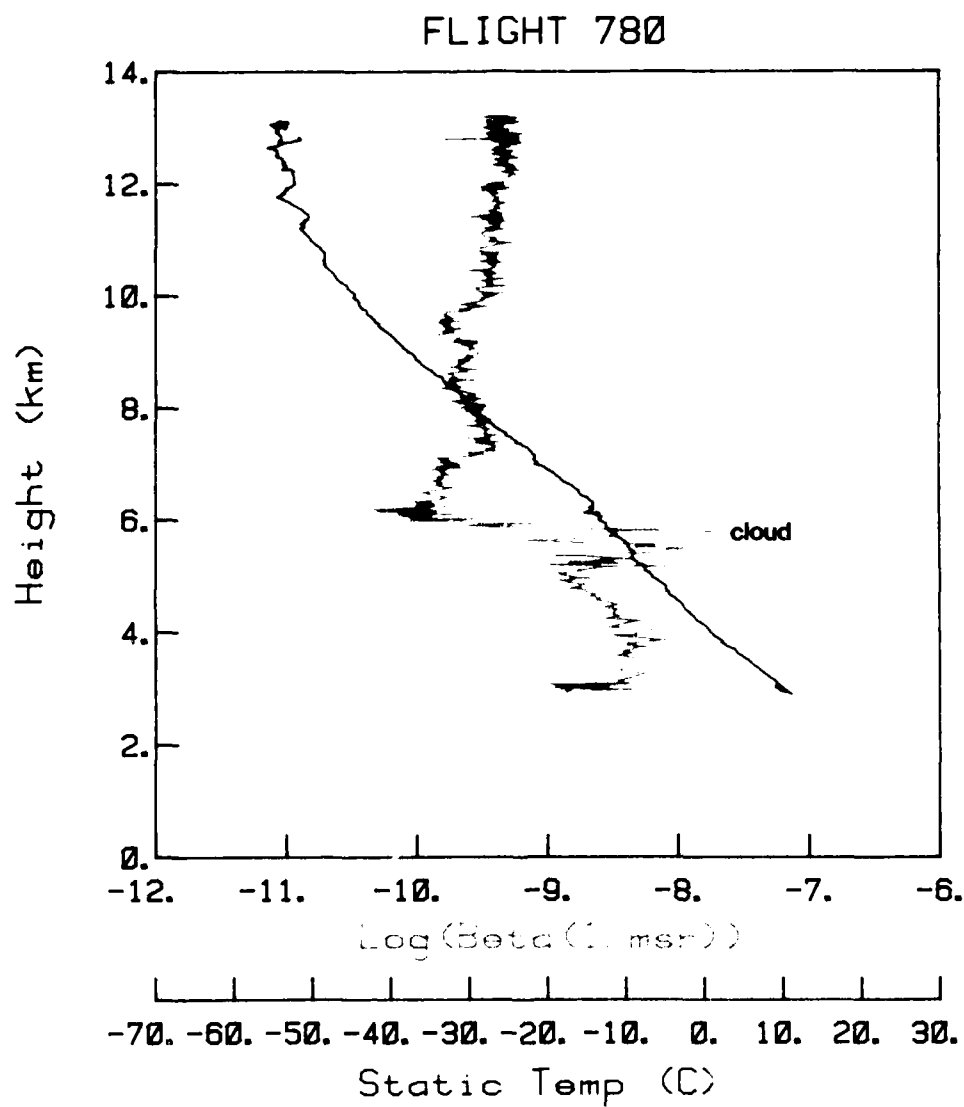


Figure 19A. Climb out of Jeffco, 9 July 1982. The observer's log records a thin layer of cloud on ascent at 5.5 km and very uniform signal above that.

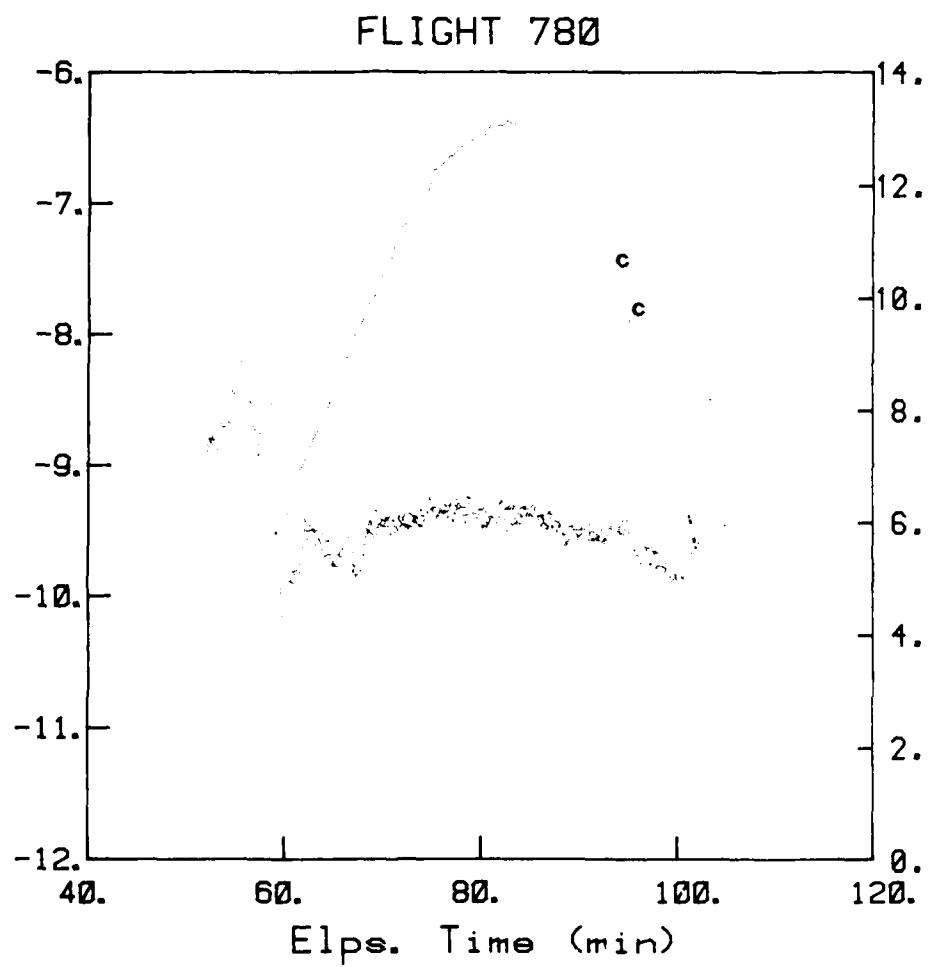


Figure 19B. Climb and descent near Jeffco, 9 July 1982. The observer's log also records passing through cloud layers c on descent at ~ 10 km as well as at ~ 6 km.

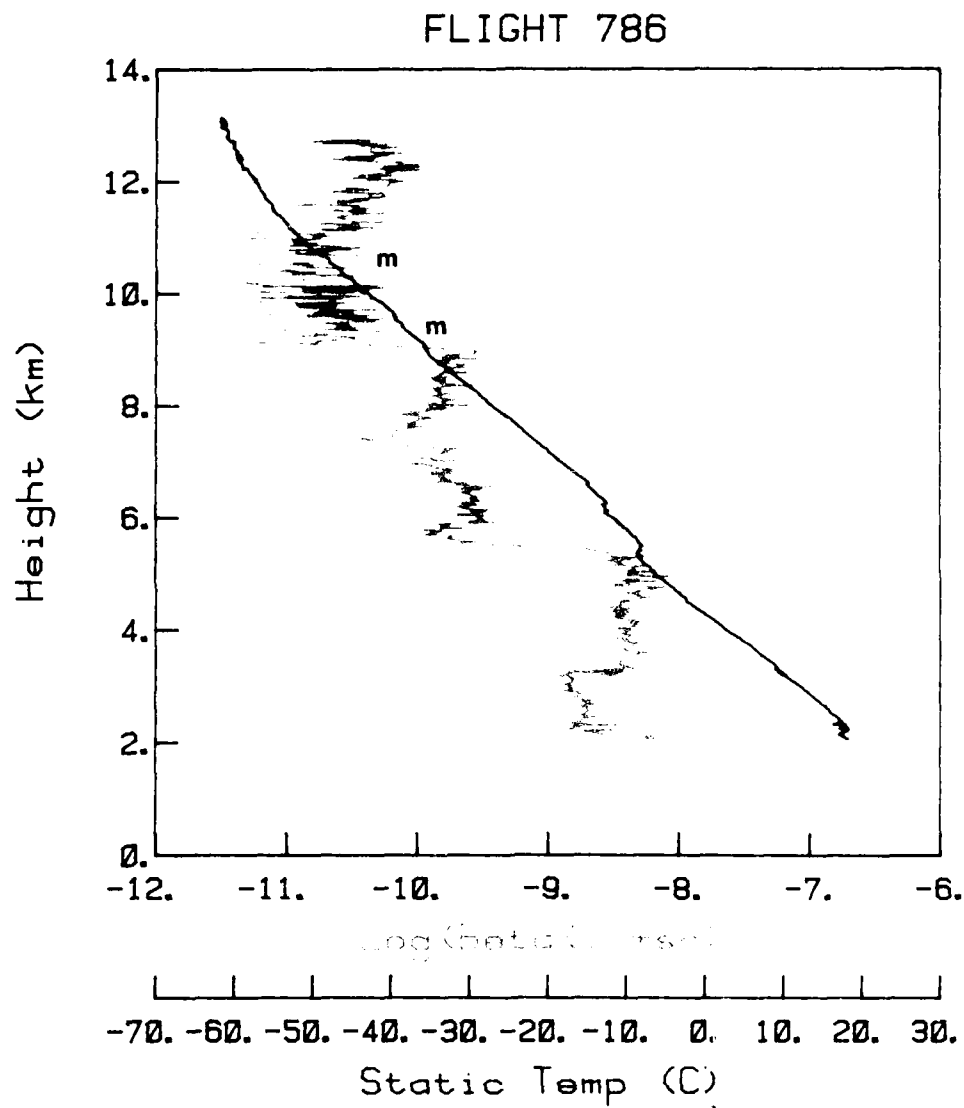


Figure 20A. Climb flying east from Jeffco, 12 July 1982. The observer's log records that signal had fallen to a very low level from ~ 9 to 11 km. Particularly in the regions marked m the level was below the minimum detectable and there are several blank experiments.

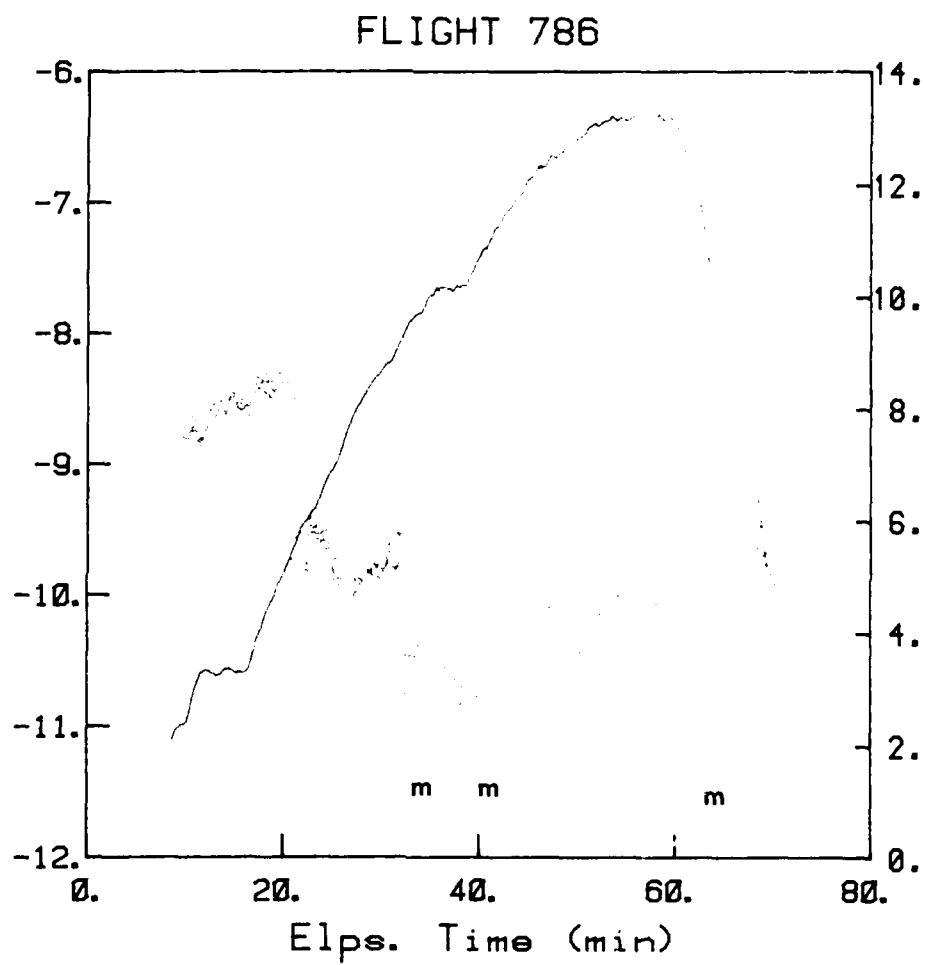


Figure 20B. Flight based on Jeffco, 12 July 1982. The signal in individual experiments was often below the minimum detectable in the height region 9 to 11 km on ascent and descent (m).

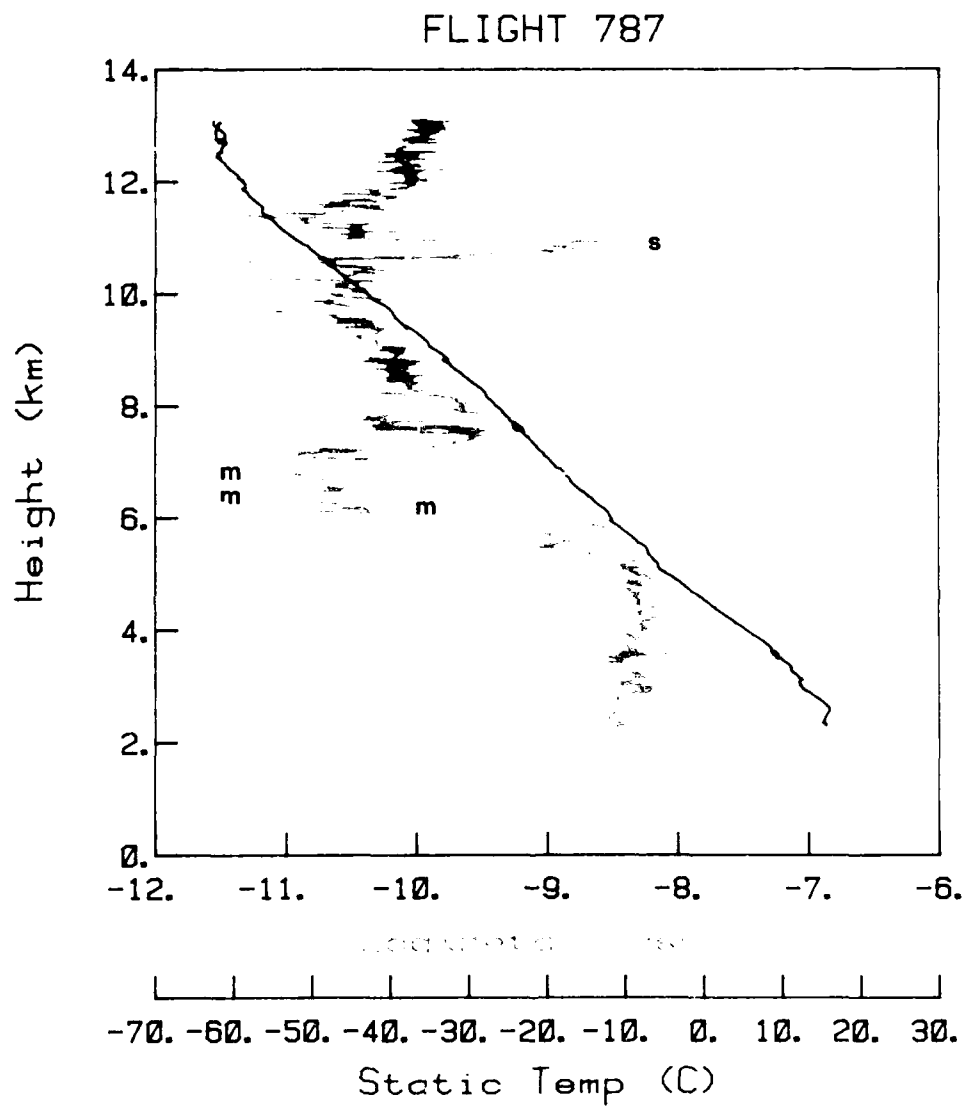


Figure 21A. Climb out of Jeffco, 13 July 1982. At 6 km altitude the backscattering fell very sharply and was occasionally below minimum detectable (m). The log records that the signal was very strong and saturating over a narrow height interval (s) at ~ 11 km with no visible cirrus; there was also the impression of a haze layer at 12.5 km.

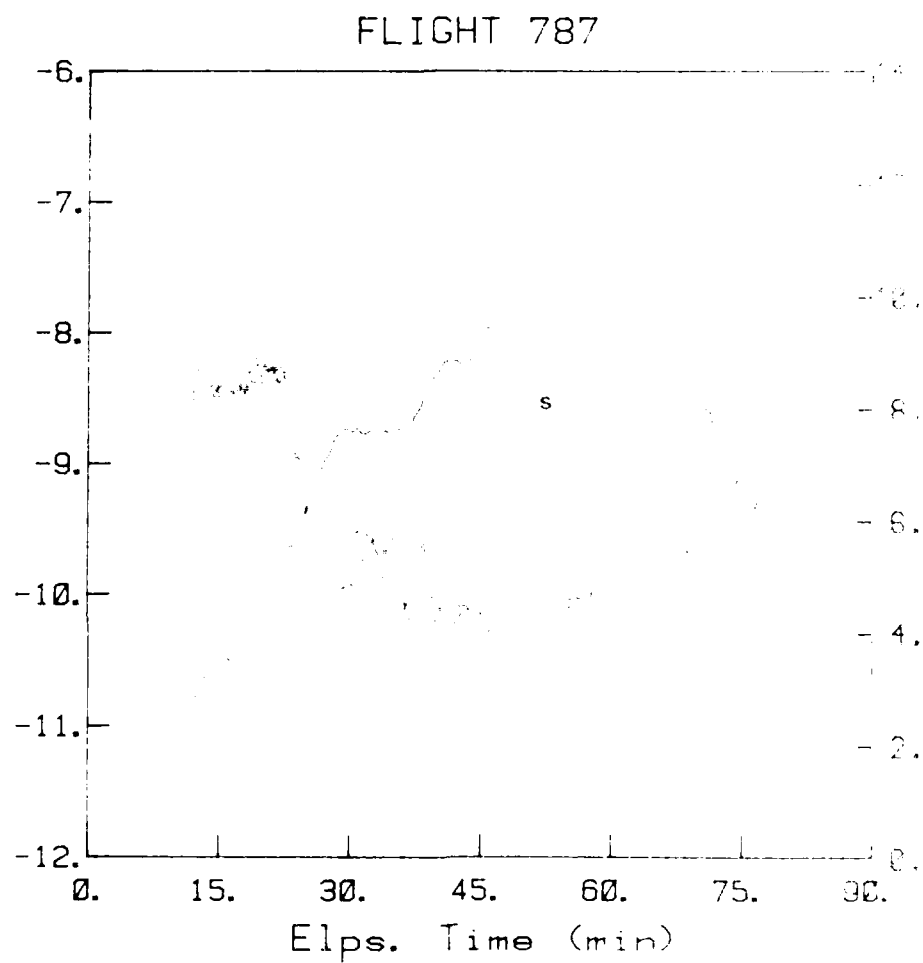


Figure 21B - Climb and rapid descent, Jettco 1, July 1980. Note the strong (and saturating) signal at s.

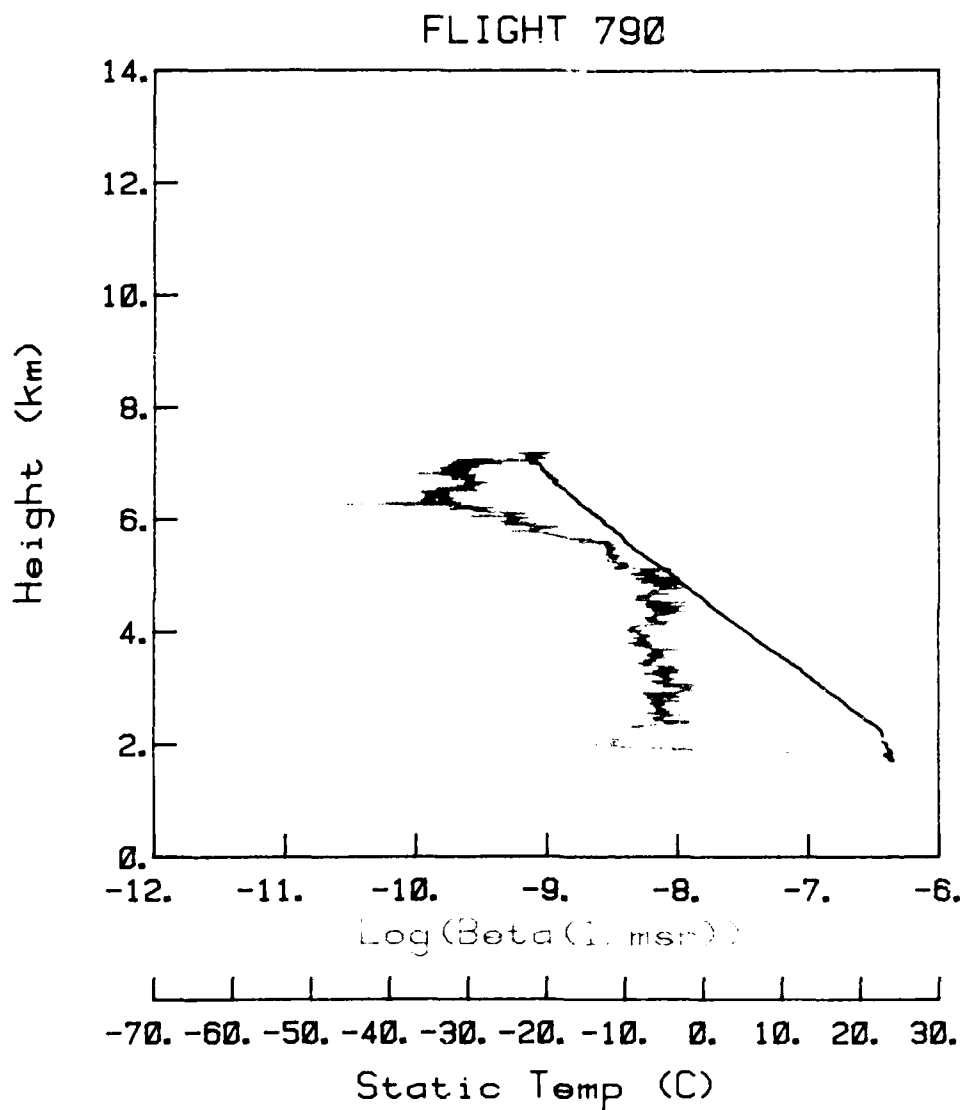


Figure 22A. Slow climb from Jeffco, 14 July 1982 in company with the King Air aircraft of NCAR. This aircraft was equipped with a particle counter capable of registering particles $> 1 \mu\text{m}$. On ascent the log records particle counts of (2-4)/10 per cc up to ~ 5 km, $[\beta(\pi) \lesssim 10^{-8} \text{ m}^{-1} \text{ sr}^{-1}]$, few or nil recorded counts at ~ 6 km $[\beta(\pi) \lesssim 10^{-10} \text{ m}^{-1} \text{ sr}^{-1}]$ and occasional 1/10 per cc at ~ 7 km $[\beta(\pi) \sim 10^{-9} \text{ m}^{-1} \text{ sr}^{-1}]$.

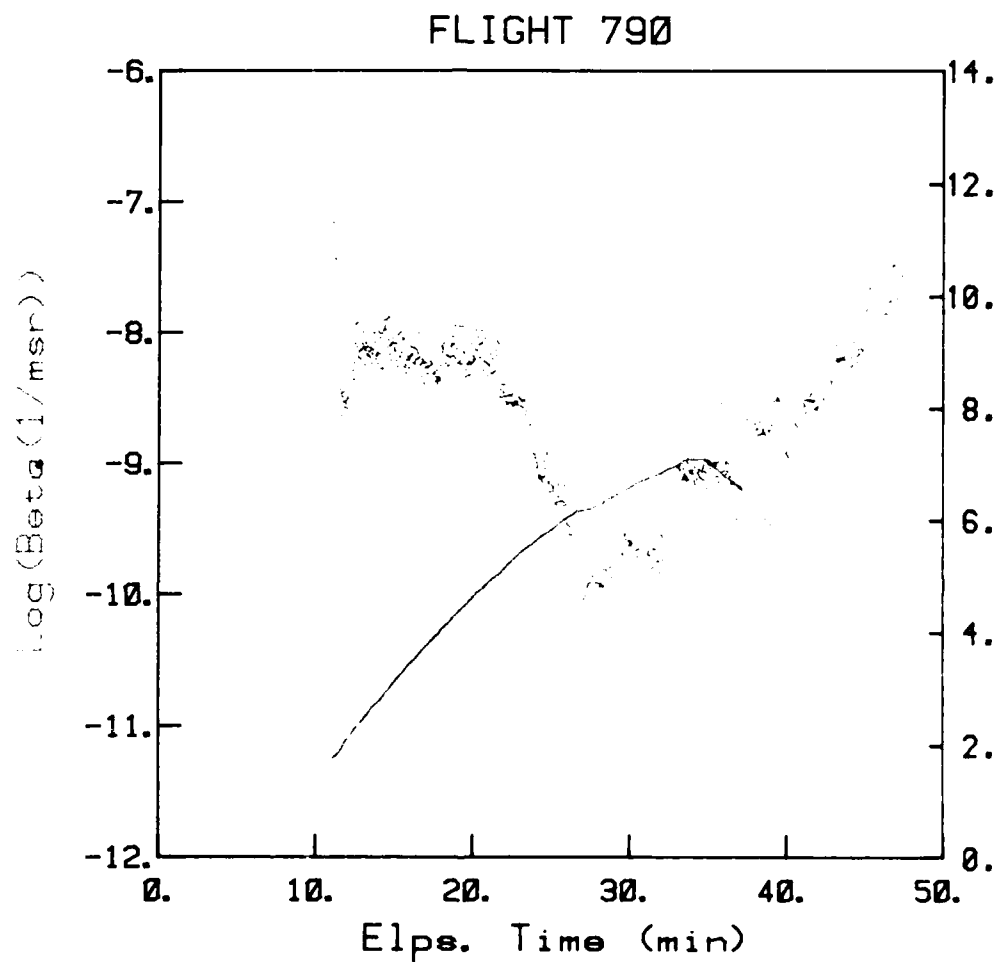


Figure 22B. Climb and descent, Jeffco, 14 July 1982 in company with the instrumented King Air aircraft of NCAR. The log records similar findings for descent: particle counts of $\sim 1/10$ per cc at 6 km [$\beta(\pi) \sim 10^{-9} \text{ m}^{-1} \text{ sr}^{-1}$] rising to (1-2)/10 per cc at 5 km [$\beta(\pi) \sim 5 \times 10^{-9} \text{ m}^{-1} \text{ sr}^{-1}$].

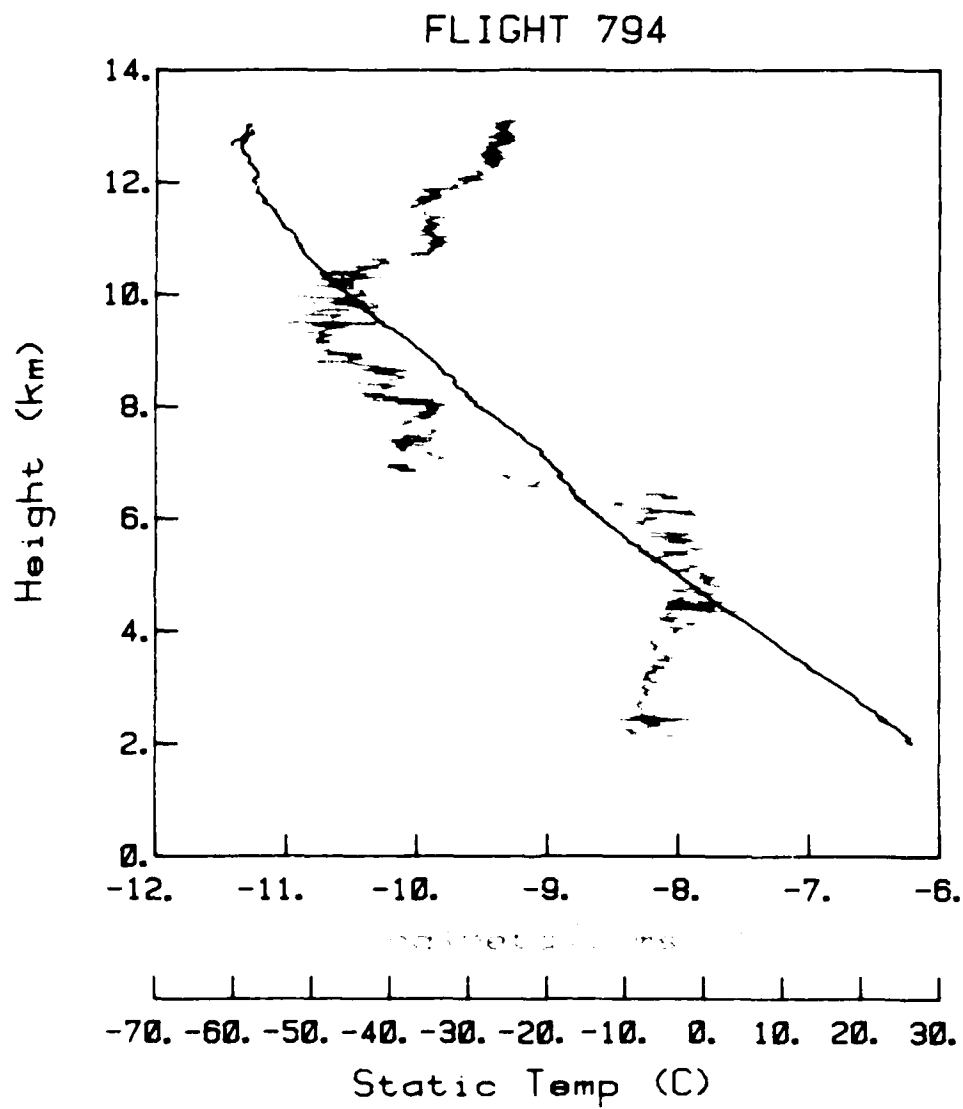


Figure 23A. Climb out of Jeffco, 15 July 1982. The log records haze to ~ 4 km altitude and the presence of alto-cumulus cloud between ~ 5 km and 6.5 km — but the aircraft did not pass through this cloud.

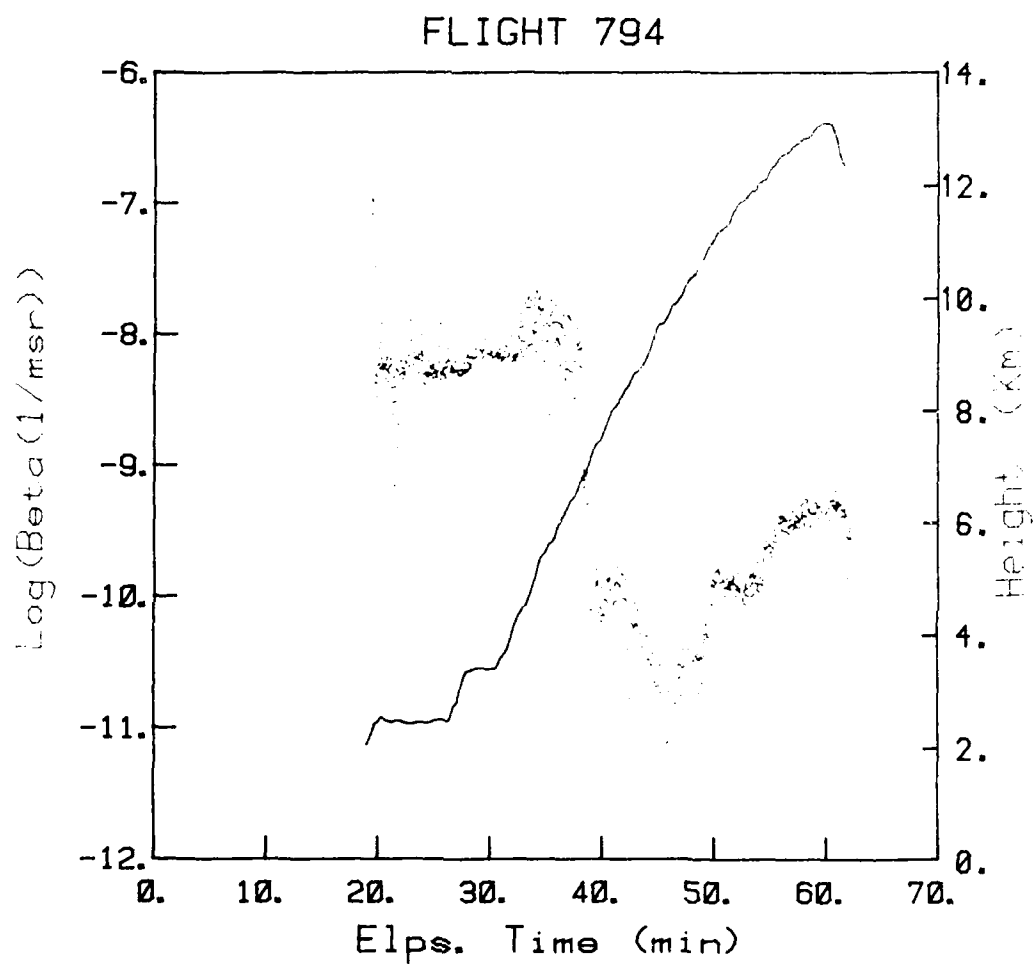


Figure 23B. Climb out of Jeffco, 15 July 1982. Only the climb portion of the flight was recorded; note the strong backscattering coefficient above 11 km — which increased steadily with altitude.

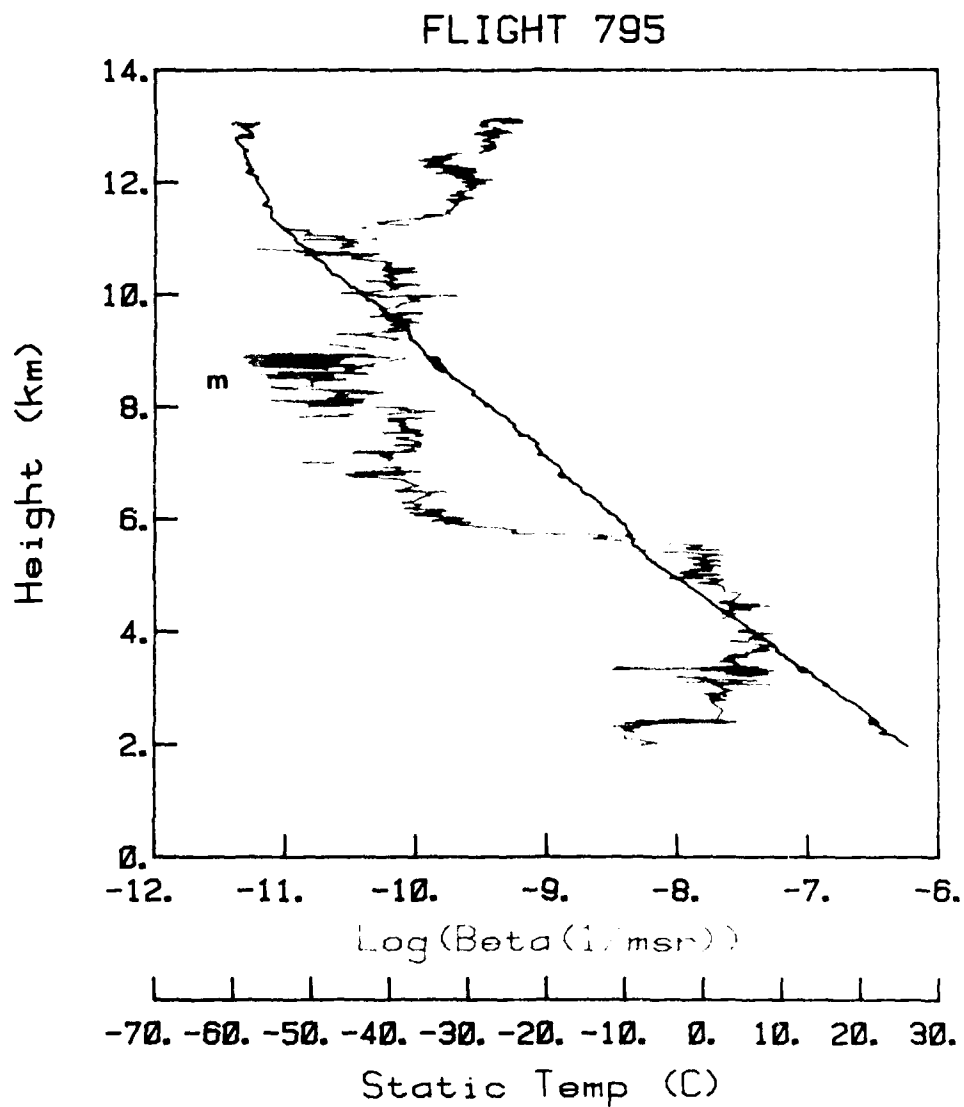


Figure 24A. Climb (with several holds) out of Jeffco, 16 July 1982. The log records clear sky, with some haze and very strong, often saturating, signal up to ~ 6 km. The signal fell to minimum detectable at ~ 8.5 km. There was a darker haze layer recorded at 12.5 km and the signal steadily increased up to 13 km.

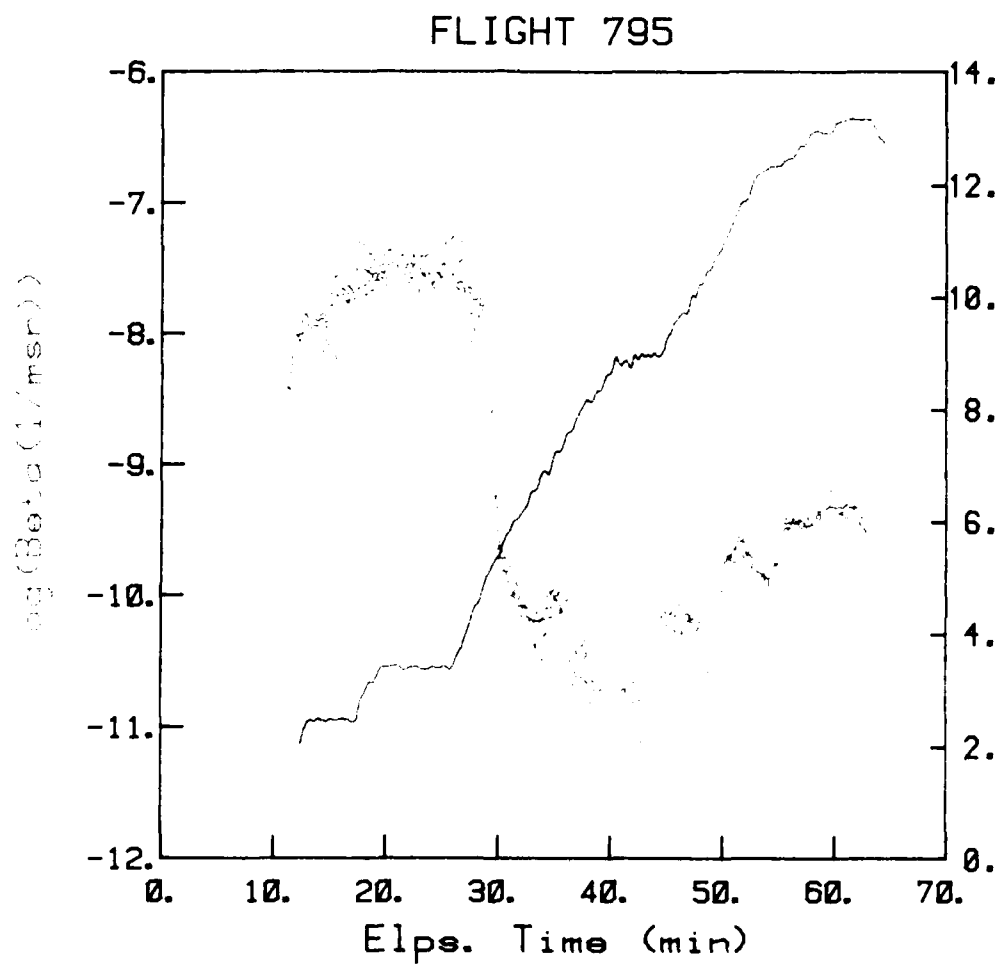


Figure 24B. Climb (with several holds) out of Jeffco, 16 July 1982. Only the climb portion of the flight was recorded. Note the similarity with the record of Flight 794 on the previous day.

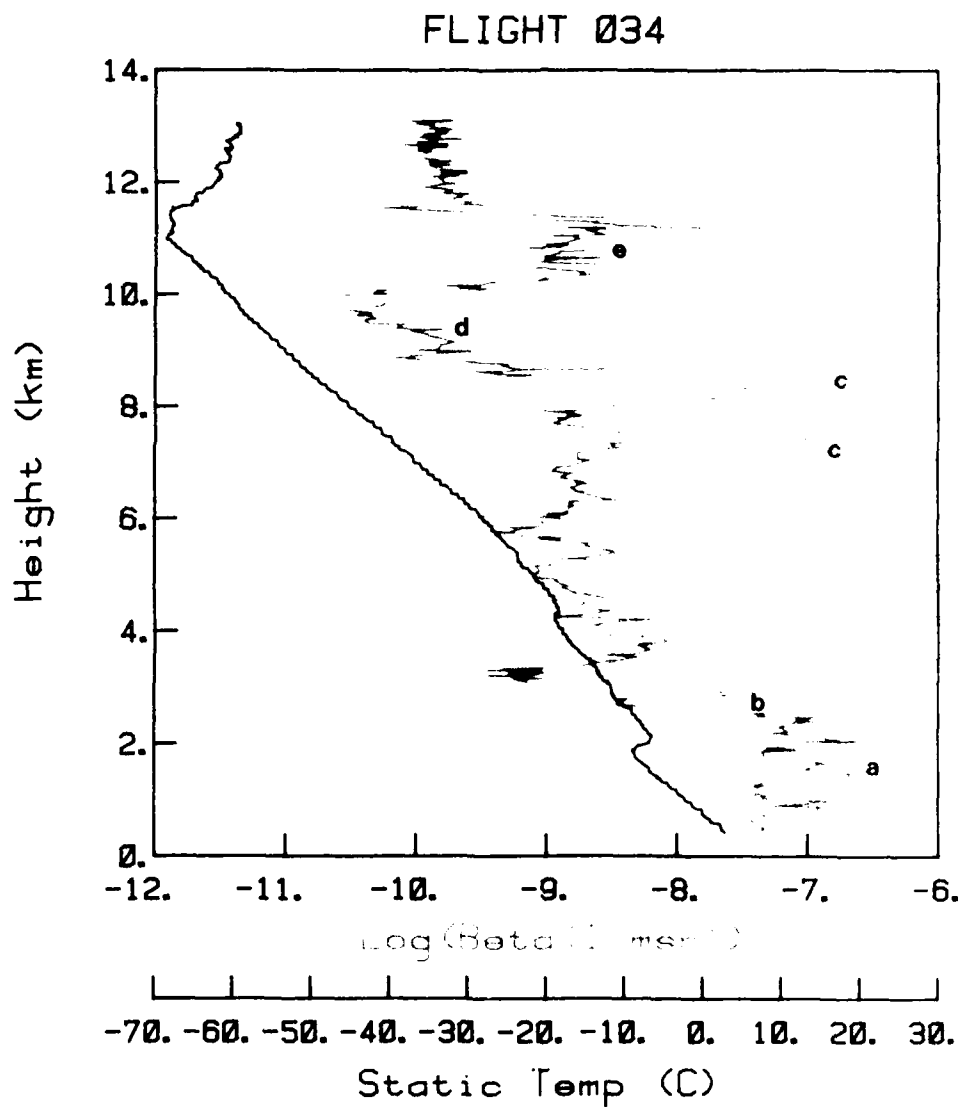


Figure 25A. Climb out of Bodo, 13 March 1986. Observer's log: a - weather hazy; b - top of haze at ~ 2.3 km; c - in slight haze and some cirrus cloud (data shows signal saturation); d - above all haze; e - no visible cloud or haze, very strong signals.

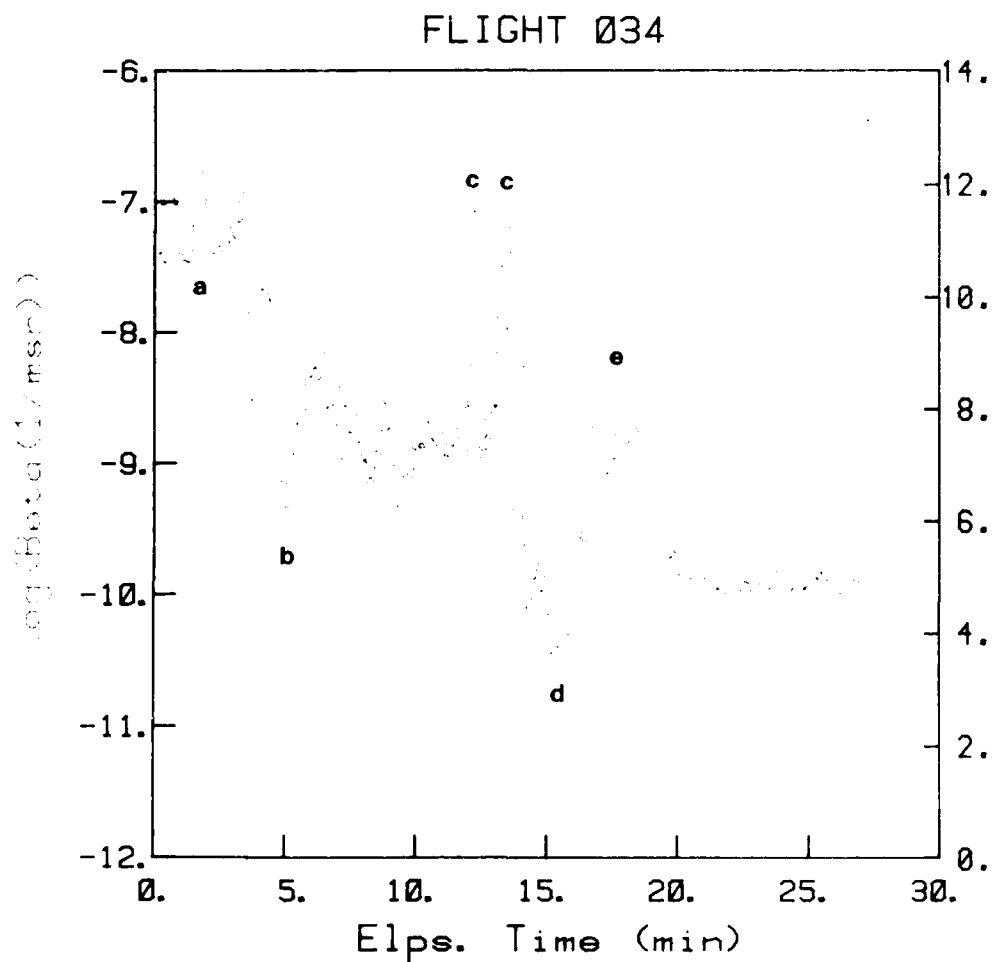


Figure 25B. Climb out of Bodo, 19 March 1986. Observer's log. a - weather hazy. b - top of haze at 2.3 km; c - in slight haze and some cirrus cloud (data shows signal saturation); d - above all haze; e - no visible cloud, very strong signal. (Note — elapsed time from start of recording). Unfortunately the data for the short transit and descent part of the flight were lost due to tape recorder malfunction.

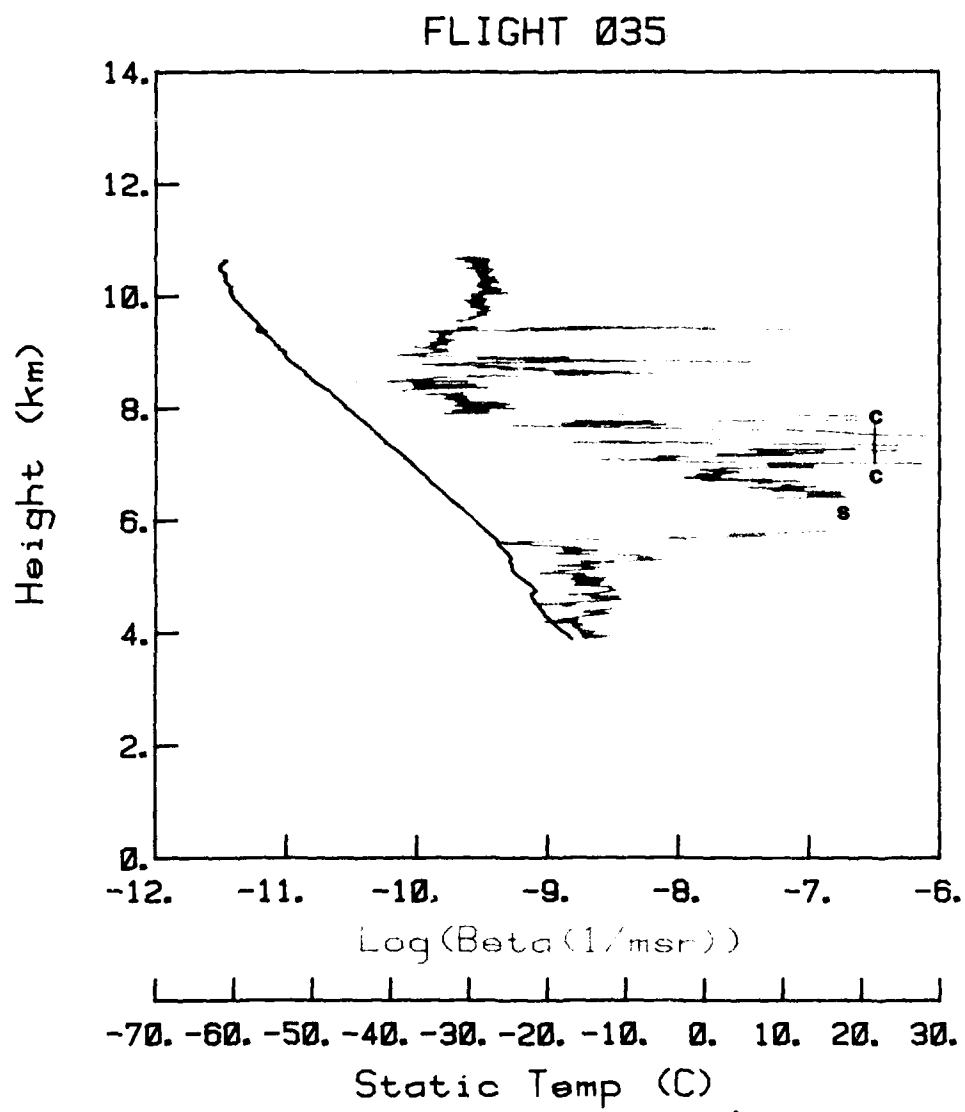


Figure 26A. Climb out of Bodo, 19 March 1986. The signal was fully saturated at s; the observer's log records in and out of thin cirrus at c, and the data shows occasional signal saturation.

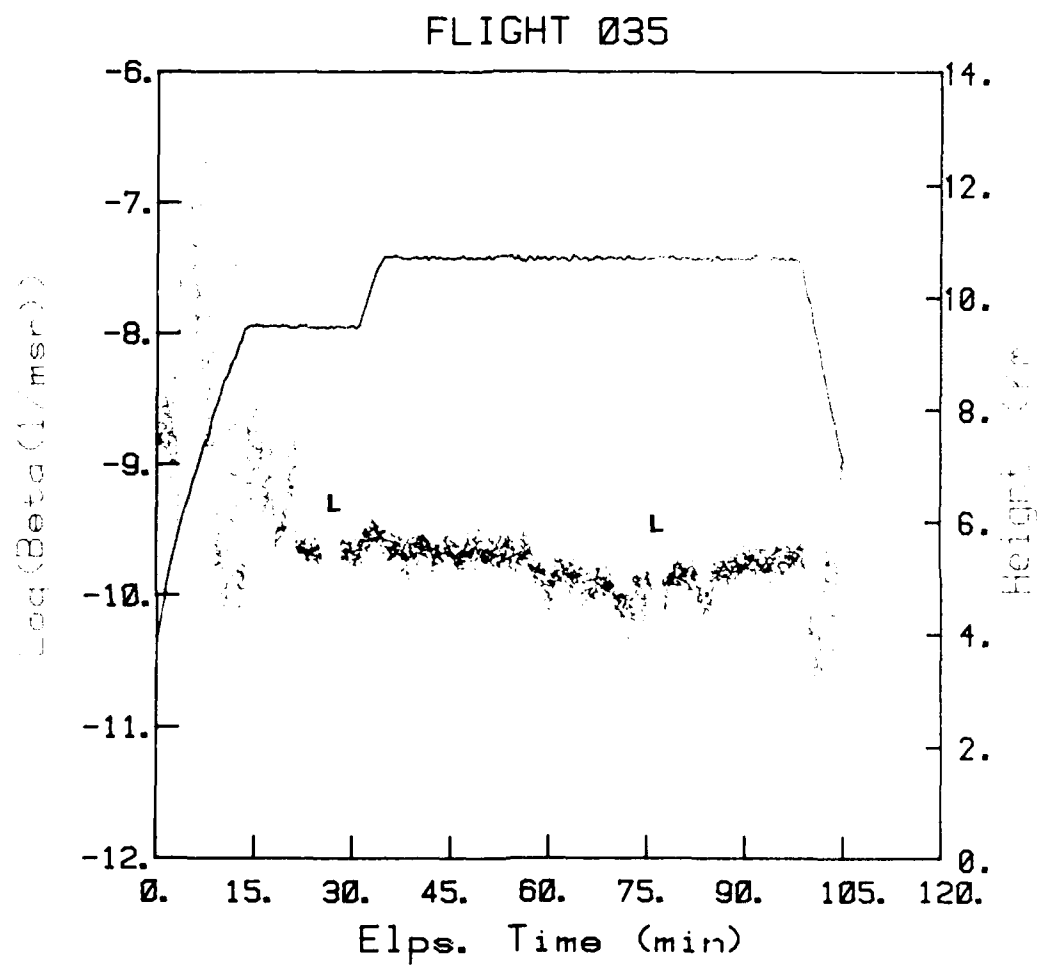


Figure 26B. Bodo to Stavanger, 19 March 1986. The few regions where the laser lost lock are indicated by an L. (Note - elapsed time from start of recording.)

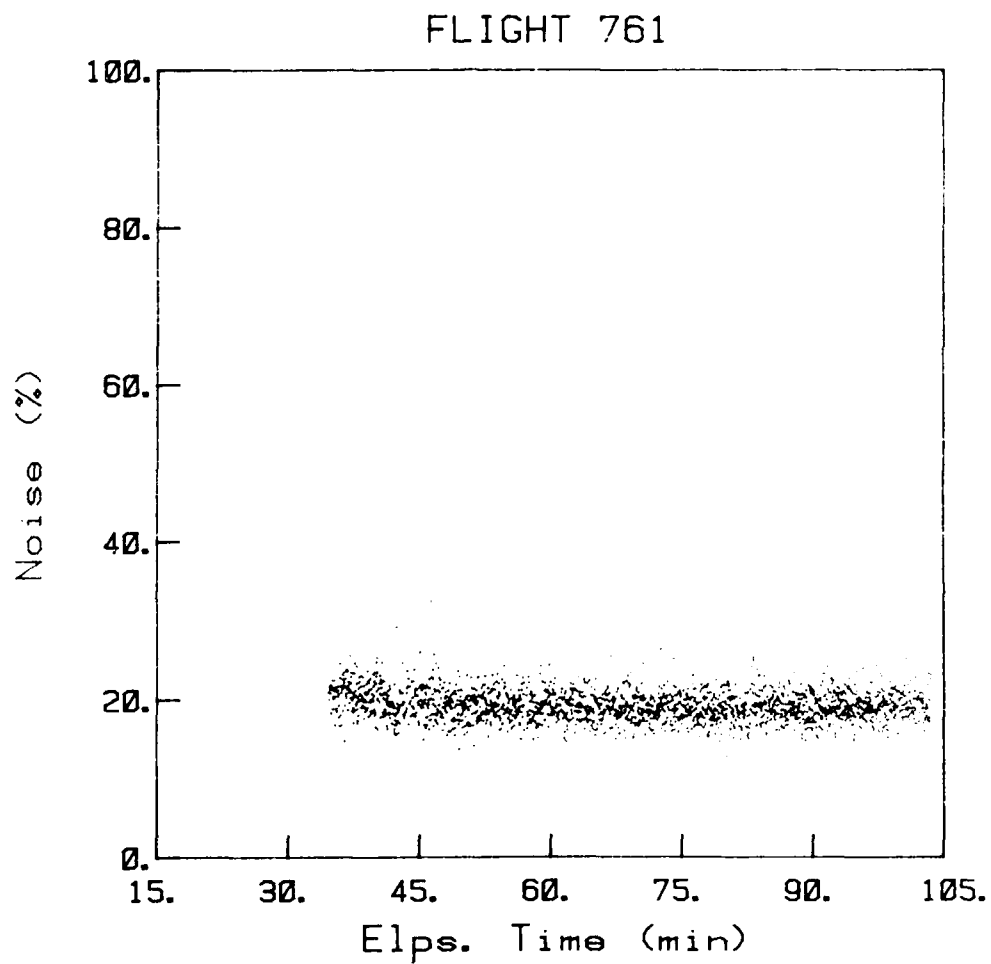


Figure 27. Level of background noise through the part of Flt 761 containing low backscatter values for the period 47-59 minutes. There is no obvious change of noise level that would indicate any equipment malfunction at that time.

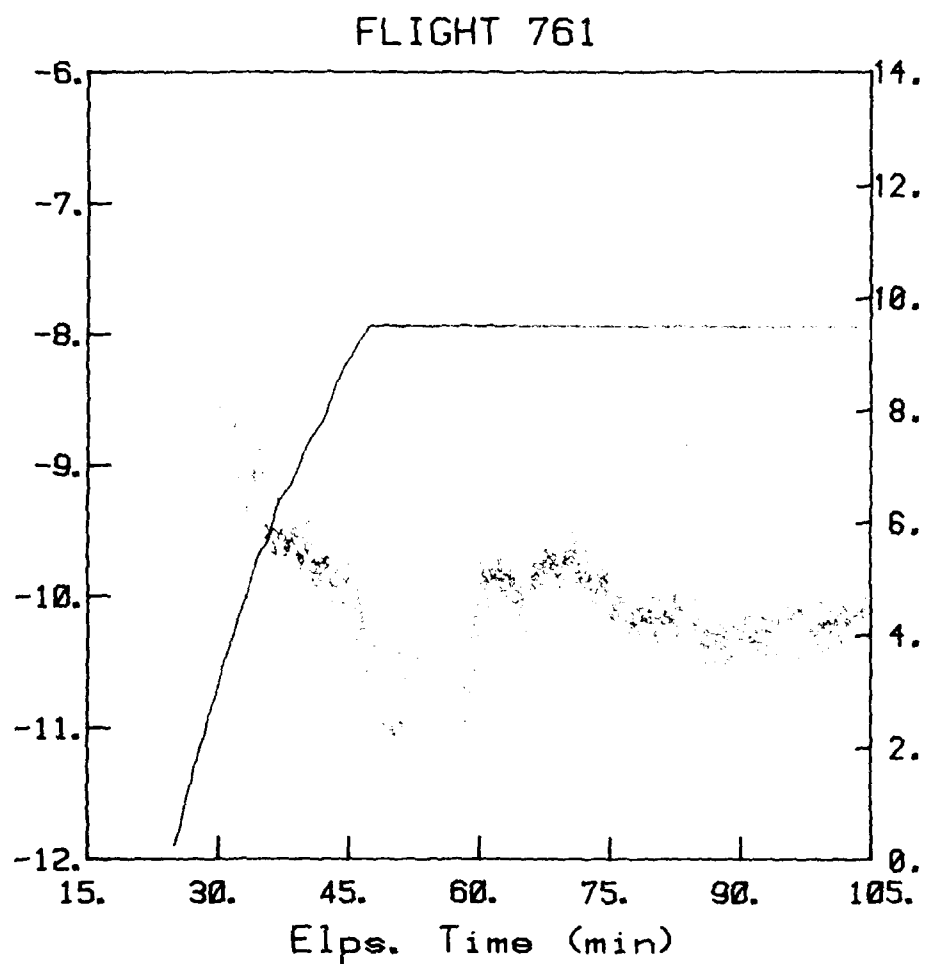


Figure 28. Re-evaluation of data shown in Figure 11B with the search window narrowed to $V_t \pm 1.5$ knots (± 5 channels). There are very few changes compared with the larger standard search window (± 3 knots) and in particular the bimodal distribution for 47-59 minutes is still evident (see discussion in text).

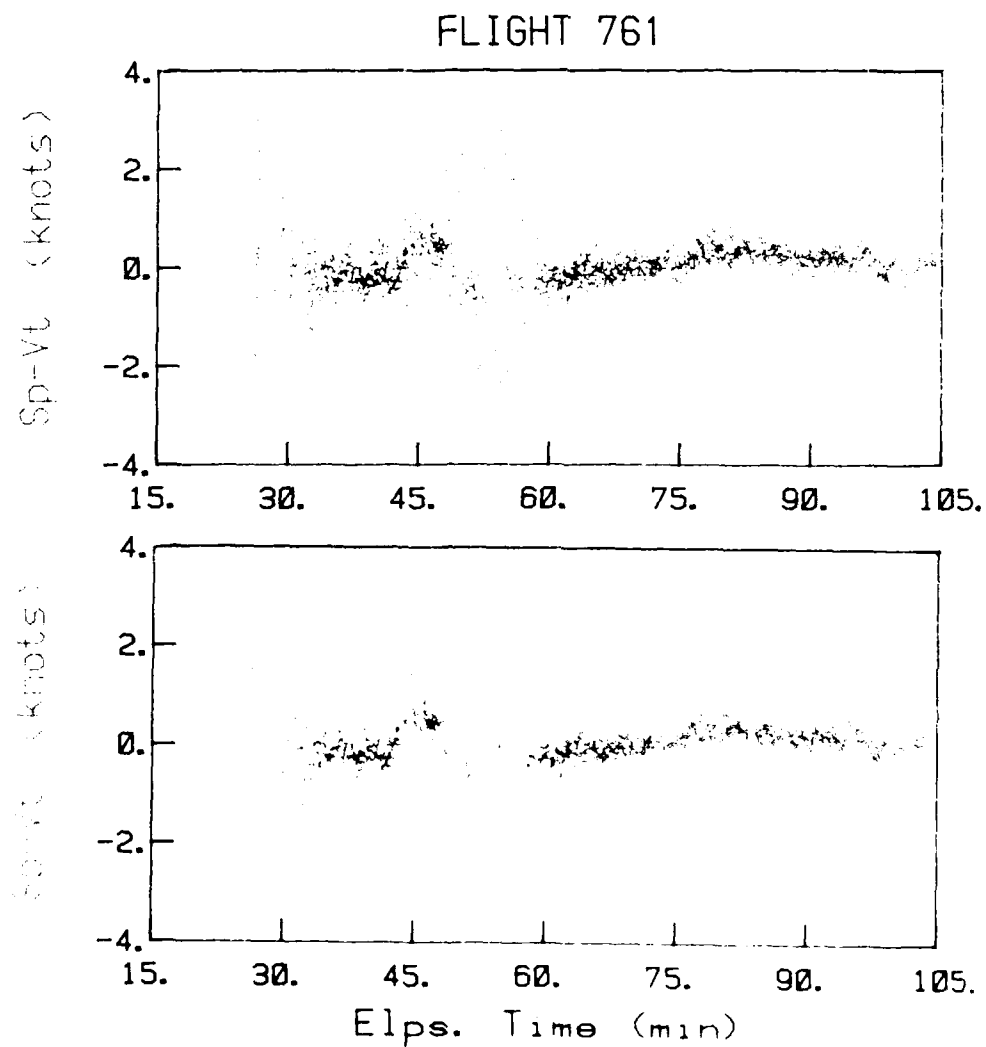


Figure 29. Plots of $S_p - V_t$ versus elapsed time for two different target velocities: a) $V_t = 3$ knots and b) $V_t = 1$ knot. Note that throughout the plot and in general, the data points are distributed almost uniformly across the y-axis with few points clustered near the origin, indicating that there are few genuine signal points in this region. After examining the data points in detail, they are identical and very close to the $S_p - V_t = 0$ line, indicating that the signal peak has been found with little uncertainty.

END

DATE
FILMED

2 88

DTIC